Atmospheric Temperature Responses to Solar Irradiance and Geomagnetic Activity

Hua Lu[a,1], Martin J. Jarvis[a], Hans-F. Graf[b], Peter C. Young[c], Richard B. Horne[a]

[a] *British Antarctic Survey, Cambridge, UK*

[b] *Centre for Atmospheric Science, University of Cambridge*

[c] *Centre for Research on Environmental Systems and Statistics, Lancaster University, UK*

Submitted to Journal of Geophysics Research

November 2006

---

[1]Corresponding author address: Hua Lu, British Antarctic Survey, High Cross, Madingley Road, Cambridge, CB3 0ET, UK

Email: hlu@bas.ac.uk

Abstract

The relative effects of solar irradiance and geomagnetic activity on the atmospheric temperature anomalies (T_a) are examined from the monthly to inter-decadal time scales. Geomagnetic Ap (A_p) signals are found primarily in the stratosphere, while the solar F10.7-cm radio flux (F_s) signals are found in both the stratosphere and troposphere. In the troposphere, 0.1–0.4 K increases in T_a are associated with F_s. Enhanced F_s signals are found when the stratospheric quasi-biennial oscillation (QBO) is westerly. In the extra-polar region of the stratosphere, 0.1–0.6 K and 0.1–0.7 K increases in T_a are associated with solar irradiance and with geomagnetic activity, respectively. In these regions, F_s signals are strengthened when either the QBO is easterly, or geomagnetic activity is high, while A_p signals are strengthened when either the QBO is westerly, or solar irradiance is high. High solar irradiance and geomagnetic activity tend to enhance each other's signatures either making the signals stronger and symmetric about the equator or extending the signals to broader areas, or both. Positive A_p signals dominate the middle Arctic stratosphere and are 2–5 times larger than those of F_s. When solar irradiance is low, the signature of A_p in T_a is asymmetric about the equator, with positive signals in the Arctic stratosphere and negative signals at mid-latitudes of the NH stratosphere. Weaker stratospheric QBO signals are associated with high A_p and F_s, suggesting possible disturbances on the QBO. The signals of A_p and F_s are distinct from the positive temperature anomalies resulting from volcanic eruptions.

1. Introduction

An 11-year solar cycle signature has been previously found in various climate parameters including surface temperature, cloud cover, rainfall, and tropical cyclones at a variety of places [*Hoyt and Schatten*, 1997]. Based on linear regression/correlation analysis between F10.7-cm radio flux (F_s) and atmospheric variables such as geo-potential height, zonal wind or temperature, the signature of the 11-year solar cycle is also found in the NCEP/NCAR and the ERA-40 reanalysis [*Crooks and Gray*, 2005; *Gleisner and Thejll*, 2003; *Haigh*, 2003; *Labitzke*, 2002]. A main feature from those reanalysis-based studies was that a positive F_s signature is present in the subtropical lower stratosphere and the signature extends into the troposphere in two near-vertical bands, one in the Northern Hemisphere (NH) and the another in the Southern Hemisphere (SH) at latitudes 20–50° [*Gray et al.*, 2005]. Most recently, *Salby and Callaghan* [2006] found that, between 1968 and 2000, atmospheric temperature correlates with the 11-year variations of F_s in the stratosphere subtropics and the F_s signals are broadly symmetry about the equator, but little solar signal can be found in the troposphere. They further revealed that the correlation is enhanced and extended to the upper and middle tropospheric mid-latitudes only if a low pass filter (~ 5 years) is applied. The tropospheric signal is, nevertheless, considerably smaller (*e.g*. below 0.1 K for annual sampling) than a number of previous studies [*Crooks and Gray*, 2005; *Haigh*, 2003].

One of the most-quoted possible mechanisms for such a solar-weather relationship is that the ultraviolet (UV) radiation modulates ozone production in the low latitude stratosphere. It is known that the solar radiation in the UV part of the spectrum varies by about 5–10% between solar maxima and minima, and plays a major role in oxygen and ozone photolysis within the stratosphere and mesosphere [*Rottman et al.,* 2004]. An increase of oxygen (ozone) photolysis leads to ozone production (decrease). These associated radiative and chemical processes cause changes in the circulation conditons of the middle and upper atmosphere and may have an indirect effect on the lower stratosphere and on the troposphere through dynamical coupling [*Haigh*, 1996; *Kodera and Kuroda,* 2002]. For instance, *Kodera and Kuroda* [2002] suggested that a solar-UV-related forcing near the stratopause may cause dynamical feedback on the lower atmosphere through a change of the Brewer-Dobson circulation and a modulation of the winter polar vortex.

By imposing realistic spectral solar irradiance variations and associated ozone variations, a number of general circulation model (GCM) simulations show that changes in upper stratospheric ozone and winds affect the flow of energy at lower altitudes [*Haigh*, 1999a; *Haigh*, 1999b; *Haigh et al.*, 2005; *Matthes et al.*, 2004; *Shindell et al.*, 1999; *Shindell et al.*, 2001]. The observed temperature anomaly of 1–2K near the stratopause from solar minimum to solar maximum can now be reproduced by the GCMs [*Gray et al.*, 2005]. However, the lower stratospheric warming in the tropics and subtropics and the seasonal progression of the poleward and downward propagation of zonal mean zonal wind anomalies in the winter hemisphere still cannot be reproduced [*Gray et al.*, 2005; *Hood*, 2004]. In a constrained GCM simulation, in which tropical stratospheric wind is relaxed to observed wind including Semi-Annual Oscillation (SAO) and Quasi Biennial Oscillation (QBO), *Matthes et al.* [2004] confirmed a crucial effect of tropical stratospheric wind on the evolution of stratospheric circulation in the northern hemisphere [*Gray et al.*, 2001]. They also showed the structure of the observed 11-

year solar cycle response in the troposphere could be reproduced with a poleward shift of the subtropical jets. Other GCM studies showed that Hadley cell weakening occurs at solar maximum in response to the warming of the tropical lower stratosphere [*Haigh*, 1999b]. However, in comparison to the observations, weaker solar signals are frequently obtained in the SH, and the positive F_s signals in the lower stratospheric tropics and subtropics remain missing. This suggests that more than one pathway may exist to convey solar influences from the stratosphere to the troposphere, and the warming in the equatorial lower stratosphere is an important feature transferring the solar signal to lower levels [*Gray et al.*, 2005].

The discrepancy between modeled and observed solar signals implies that the GCMs may be missing an important mechanism [*Callis et al.*, 2000; *Rozanov et al.*, 2005]. By comparing results from the same model with the different imposed ozone distributions, *Matthes et al.* [2004] have shown that the modeled temperature response was very sensitive to the imposed ozone changes. In contrast to the heating effects of solar irradiance, coronal mass ejections, the result of momentous disruption of magnetic structures in the Sun's corona, cause a high-speed burst above the ambient speed of the solar wind. The solar wind interacts with the Earth's magnetosphere and these disturbances cause geomagnetic activity. Studies suggest that geomagnetic activity can influence the Earth's atmosphere via energetic particle precipitation (EPP) [*Callis et al.*, 1991; *Randall et al.*, 2005; *Siskind et al.*, 2000; *Solomon et al.*, 1982]. Examples of ionization by EPP are relativistic electron precipitation events during geomagnetic disturbances [*Thorne and Larsen*, 1976] and solar proton events [*Jackman and McPeters*, 2004]. Through dissociation and ionization processes, EPP leads to routine production of odd nitrogen (NO_x) in the mesosphere (EPP, > 100 keV electrons, > 1 MeV protons) and thermosphere (EPP, < 100 keV electrons, < 1 MeV protons), and to sporadic production of NO_x directly in the stratosphere when extremely high energetic particles are involved. During the polar winter NO_x can survive for more than one month, and in the presence of a strong polar vortex, descend into the stratosphere [*Siskind et al.*, 2000; *Solomon et al.*, 1982]. Once the descending NO_x reaches the stratosphere, it persists for a much longer time, and plays a major role in the ozone balance of the stratosphere because it destroys odd oxygen ($O + O_3$) through catalytic reactions [*Brasseur and Solomon*, 1986]. For instance, *Randall et al.*[2005] reported unprecedented levels of spring-time stratospheric NO_x in the NH during 2003-2004, and several studies suggested it was a result of a high level of geomagnetic disturbances during early-mid winter and a strong late winter vortex [*Clilverd et al.*, 2006; *Renard et al.*, 2006; *Rinsland et al.*, 2005]. *Rozanov et al.* [2005] show that the magnitude of the temperature response to energetic electron events can potentially exceed the effects from solar UV fluxes, particularly in the lower part of the atmosphere in high latitudes. Using a middle atmospheric mechanistic model, *Arnold and Robinson* [2001] show that geomagnetic activity caused by solar magnetic flux forcing can influence planetary wave propagation, perturb the winter stratosphere significantly and produce a stronger subtropical winter jet in the mesosphere and upper stratosphere. Correlative studies also reveal statistically significant signals of solar wind related parameters in the atmosphere [*Boberg and Lundstedt*, 2002; *Bochnicek et al.*, 1996; *Bucha and Bucha*, 1998; *Thejll et al.*, 2003].

Both observational and modeling studies have found that the equatorial stratospheric QBO has substantial influence on the zonal circulation of the stratosphere [*Baldwin et al.*, 2001; *Holton and Tan*, 1980; *Pascoe et al.*, 2005]. *Holton and Tan* [1980] discovered that when the QBO at 50 hPa is easterly, the northern polar vortex is more disturbed and warmer, and sudden stratospheric warmings (SSWs) are more likely to occur. They speculated that the phase of the QBO affects the position of the zero wind line and appears to modulate the effectiveness of planetary waves in either strengthening or weakening the polar vortex. When the equatorial winds are easterly, planetary waves tend to propagate higher and more poleward than when the QBO is in its westerly phase. For the months around solstice, studies show that the spatial characteristics of F_s signals tend to change from one QBO phase to another both near the equator and in the polar region of the stratosphere [*Labitzke*, 1987; *Labitzke*, 2004; *Labitzke and van Loon*, 1988; *Labitzke and van Loon*, 2000; *Matthes et al.*, 2004; *Naito and Hirota*, 1997]. *Labitzke and van Loon* [1988] revealed that the temperatures within the stratospheric winter vortex are positively (negatively) correlated with the 11-year SSC when the QBO at 45 hPa is in its westerly (easterly) phase, respectively. At mid-latitudes, they observed the opposite correlations. Their recent studies show such QBO phase dependent correlation is generally true in both hemispheres and for all-year-round data [*Labitzke*, 2004; *Labitzke and van Loon*, 2000; *van Loon and Labitzke*, 1998]. More recently, *Salby and Callaghan* [2006] confirmed those earlier findings that enhanced correlations are obtained if the data are sampled at around solstice (February / August) and grouped into QBO easterly/westerly phases.

The evidence in the literature suggests that the solar influences on the atmosphere are of multiple sources and may have more than one pathway. Nevertheless, no study has yet been taken to evaluate the relative contribution of solar irradiance and geomagnetic activity. Previous studies all concentrated on only one form of solar forcing and the atmospheric responses to solar irradiance and geomagnetic activity were investigated in isolation. Differences in data, analytical methods, and time scales and period, etc make it impossible to assess the relative influences of solar irradiance and geomagnetic activity directly from those previous studies. One primary objective of this paper is to examine the difference and relative influences of solar irradiance and geomagnetic activity on the Earth's climate using the same atmospheric data, with the same evaluation criteria and analytical methods.

This study represents a first step towards understanding *multiple* solar influences on the atmospheric temperature. It builds on those earlier works and is novel and distinctive in three respects. Firstly, by using a newly-available radiosonde-based global coverage of temperature anomaly (T_a) (see section 2 for details), we assess the relative effects of solar irradiance (F_s) and geomagnetic activity A_p on the global temperature anomaly from 1000 hPa to 30 hPa by detecting their signatures in T_a using linear correlation and composite analysis. Secondly, we test if the correlations are significant and the patterns are stable by using different filtering windows and different time periods. Thirdly, we study, at the inter-annual time scale, the mutual-modulation relationships among QBO, solar irradiance and geomagnetic activity by sub-sampling the data according to the phases of QBO, the strength of solar irradiance and the level of geomagnetic activity, respectively. There are two underlying hypotheses for the entire paper. That is, the quasi-decadal variations (QDVs) found in the previous literature are the results of multiple solar forcing; and the atmospheric responses to the solar influences may be modulated by the stratospheric QBO and can be treated piece-wise-linearly in terms of the intensity of solar irradiance and geomagnetic activity.

2. The Data and Methods

Four major data sets are used in this study. Solar irradiance appears concurrently in the TSI and the UV irradiance, though solar UV irradiance may intrinsically have much larger amplitude of variation in the interannual to decadal time scales than TSI [*Lean et al.*, 1997]. Solar irradiance was not directly measured for the entire period from 1958 to 2001, so a suitable proxy was used, *i.e.*, the 10.7-cm solar radio flux (F_s) is employed [*Hinteregger*, 1981]. It is known that F_s originates from atmospheric layers high in the Sun's chromosphere and low in its corona, and responds primarily to changes in the solar faculae that are mainly responsible for emitting the UV radiation [*Lean*, 1991]. In general, high/low F_s corresponds to solar maximum/ minimum conditions, respectively. The monthly averaged F_s are downloaded from the National Geophysical Data Center (NGDC) website (www.ngdc.noaa.gov/stp/SOLAR). It is worth noting that though solar UV irradiance may be more effective in generating and modulating responses on interannual to decadal time scales, the multidecadal and longer-term response in earth's atmosphere are more likely associated with the persistent forcing by TSI. However, either F_s or the 44-years of temperature anomaly data used here cannot capture those longer-term responses.

The Ap index is a measure of geomagnetic storm activity over the globe [*Mayaud*, 1980]. It is derived from measurements made at a number of stations world-wide of the variation of the geomagnetic field due to currents flowing in the earth's ionosphere. It measures the energy deposited in the Earth's upper atmosphere by charged particle bombardment induced by the solar wind, and is largely affected by the variations in solar plasma flux, which affects the solar wind as well as interplanetary magnetic field parameters. The Ap index is found to be highly correlated with solar wind velocity and low Ap values indicate a quiescent interplanetary medium as well as low solar wind speed [*Garrett et al.*, 1974]. Large Ap values are often associated with an increase in the number of coronal holes that produce an unrestricted outward flow of solar plasma into interplanetary space and a subsequent disturbance to the Earth's magnetic field [*Sheeley et al.*, 1976]. Geomagnetic activity tends to peak during the descending phase of solar cycles when the high-speed solar wind streams are highly recurrent and most intense [*Vennerstrom and Friis-Christensen*, 1996]. Studies have suggested that the Ap index is a good indicator of upper atmospheric EPP [*Randall et al.*, 1998]. *Siskind et al.*[2000] examined the year-to-year NO_x variability of the total column inside the SH stratospheric vortex. These authors found that, while month-to-month correlation is poor, the average column NO_x inside the vortex during May to August for 1991-1996 is well correlated to 4-month averaged Ap index. Studies have also suggested that this is due to an accumulative effect of low energy particle precipitation generated by smaller, but more continuous geomagnetic storms occurring primarily in the thermosphere [*Clilverd et al.*, 2006; *Orsolini et al.*, 2005; *Randall et al.,* 2005]. The time required for the NO_x to descend from the thermosphere to the stratosphere is, thus, in the order of 1-3 months, sometimes even longer. Other processes such as solar proton events which produce strong impulsive ionization episodes and are able to directly penetrate into the stratosphere can also be considered as a cause of the stratospheric high-altitude NO_x [*Jackman and McPeters*, 2004]. However, such very energetic events are few and should not be considered as a dominant source for stratospheric NO_x enrichment [*Lean et al.*, 1997; *Solomon et al.*, 1982]. To account for the delayed response to geomagnetic activity, for all the case studies presented here, a 2-month forward lag is applied to the Ap index. The lagged time series is denoted as A_p and used throughout the paper. There are still large uncertainties in identifying the causes and the precise source regions of the stratospheric descent of NO_x and the 2-month forward lag applied to the Ap index may not represent the precise time lag for stratospheric NO_x caused by geomagnetic activity. Nevertheless, such a time lag is adequate for the inter-annual to inter-decadal time scales under investigation. The monthly averaged Ap index is available from 1932 to the present time and is downloaded from the National Geophysical Data Center website.

Figure 1 shows the time series of monthly mean F_s and A_p. It shows, A_p peaks at different times in comparison to that of F_s. The first A_p peak often occurs slightly before solar maximum, while the second and more intense peak occurs during the declining phase of F_s. in comparison to F_s, the temporal variation of A_p is more rapid.

[Insert Figure 1 here]

Radiosonde observations of stratospheric equatorial winds are available monthly since 1956 at 7 pressure levels from 70 to 10 hPa [*Naujokat*, 1986]. The magnitude of correlations involving extra-tropical fields depends on the exact level chosen to define the QBO. In the northern hemisphere (NH), the strongest extratropical signals were obtained using a level near 40–50 hPa; while the magnitude of the southern hemisphere (SH) response appears to be maximized using 20–30 hPa [*Baldwin and Dunkerton*, 1998]. In this study, the QBO phases were determined by the direction of the averaged zonal wind at 40 to 50 hPa. There is, therefore, a bias towards the NH.

The temperature anomaly data set we used is the zonally averaged T_a (relative to the monthly 1966-95 climatology) from the Hadley Centre referred to as HadAT2. This is a recent analysis of the global upper air temperature record from 1958 to present based upon radiosonde data alone [*Thorne et al.*, 2005]. The source data set consists of 676 pre-selected radiosonde stations, which were quality controlled to ensure that both spatial and temporal consistencies are maintained. Though the data have missing values in the SH and a bias towards NH mid-latitudes, it is probably one of the most reliable temperature anomaly measurements available [*Thorne et al.*, 2005]. The monthly data are available on a 5° latitude resolution at nine separate pressure levels (850, 700, 500, 300, 200, 150, 100, 50, and 30hPa). The HadAT2 is merged with the monthly, zonal averaged surface temperature anomaly from HadCRUT2V (http://www.cru.uea.ac.uk/cru/data/temperature/) sub-sampled to the same period to represent 1000 hPa data. A common time period shared by these four data sets (*i.e.* F_s, A_p, QBO, and T_a) is from Jan. 1958 to Dec. 2004, thus covering 4 solar cycles.

To understand the mutual-modulating effects among solar irradiance, geomagnetic activity and the QBO, the monthly data are sub-sampled according to the phases of QBO (*i.e.* westerly or easterly) and the phases of solar irradiance (*i.e.* high or low F_s), or the levels of geomagnetic activity (*i.e.* high or low A_p), respectively. We use the normalized time series of QBO, F_s and A_p to define those phases and the same threshold value of 0.15 is applied for all three normalized time series. That is, $\overline{QBO} <$ -0.15, $\overline{QBO} > 0.15$ $\overline{F_s} < -0.15$, $\overline{F_s} > 0.15$, $\overline{A_p} < -0.15$, and $\overline{A_p} > 0.15$ defines easterly QBO, westerly QBO, low solar irradiance, high solar irradiance, low geomagnetic activity, and high geomagnetic activity, respectively, where $\overline{QBO}$, $\overline{F_s}$ and $\overline{A_p}$ are normalized values of QBO, F_s and A_p. For a given sample, the signals of the QBO, F_s, and A_p are studied by performing linear correlations between those three normalized time series and T_a, respectively. We check if the correlations are stable by sampling data from different periods. In brief, we call a correlation pattern robust if: the correlations are statistically significant at a confidence level 95% or above; the spatial pattern covers 10° in latitude continuously (*i.e.* two horizontal grid points) or above; and is stable for different periods.

To investigate how the correlation pattern may vary with time scales, recursive fixed interval smoothing, based on an integrated random walk plus noise model for signal analysis [*Young et al.*, 1991], is used as either a low-pass or high-pass filter. Two types of high-pass filter are used to remove the long-term trends. One is the Integrated Random Walk SMoothing and decimation method (IRWSM) available in the CAPTAIN Toolbox [*Young et al.*, 2004]. Another is a piece-wise linear model with the breaking points pre-defined at the months of three major volcanic eruptions (Mt. Agung in March 1963, El Chichón in April 1982, and Mt. Pinatubo in June 1991, when temperatures rise abruptly), or 2-years following the eruption (in cases where observations for the three 2-year periods following major volcanic eruptions are excluded). The IRWSM method allows the user to define the cutoff period, so it is used as a low pass filter as well. A 50-year cutoff period is applied to the IRWSM method for the cases when the two years following the major volcanic eruptions are included, while the piecewise linear model is applied to the cases when the years affected by the major volcanic eruptions are excluded. We choose not to use the simple linear detrending; this is because the T_a time series are non-stationary, show abruptly temperature rises due to the major volcanic eruptions, and encompass non-linear trends. *Seidel and Lanzante* [2004] demonstrated that simple linear detrending may over-estimate the amount of temperature changes associated with the long-term trends, and the sloped steps and piecewise linear models which account for abrupt changes offer a better fit to the observations. The detrending method used by this study is an alternative but essentially similar method to those used by *Seidel and Lanzante* [2004].

Given the high degree of serial correlation in the low-pass filtered time-series, we use the non-parametric test of *Ebisuzaki* [1997]. The method is based on random phase test of one of the time series in the frequency domain thus preserving its power spectrum characteristics. For each pair of time series to be correlated, 10,000 synthetic random time series having the same power spectrum as one of the original time-series (*e.g.* F_s, A_p or QBO) and correlated them with the other original time-series (*i.e.* temperature anomaly T_a). The linear correlation coefficients are ordered in ascending order and a distribution of correlation is constructed. This distribution of correlations was compared to the original correlation and used to determine the significance levels, *e.g.*, the upper 5% tail gives the one-tailed 5% level of significance.

Serial correlation is not a serious issue for the monthly temperature anomaly (T_a) time series as low-pass filters are not applied for the composite analysis. However, the assumptions of normality and equal variances, required by the standard two-sample *t*-test, can hardly be satisfied by all the T_a time series. In this case, the significance level for the difference between the mean values of two composite sub-samples is estimated using a Monte Carlo trial based non-parametric test. The procedure is to select two sub-samples from the original time series with the lengths equal to the two composite sub-samples and then the difference between their mean values is computed. This procedure is repeated 10,000 times and a distribution of the differences is constructed. The composite difference is then compared to this difference distribution and the rank of the actual difference among these randomized trials determines its significance level.

The significance levels calculated using the non-parametric test of *Ebisuzaki* [1997] and Monte Carlo trials are compared to those using the standard *t*-tests and using the method of *Davis* [1976], which based on the concept of Effective Sample Size (ESS). We found that the *t*-tests give much more liberal significance levels than those where non-parametric tests were used. The method of *Davis* [1976] produces comparable results to those from the non-parametric tests, but only if the number of the lags used for calculating cross-correlations is set as around 60 months (equivalent to 5 years). As pointed out by *Thiebaux and Zwiers* [1984], we found that the ESS required by the method of *Davis* [1976] cannot be estimated consistently as its values largely depend on the number of the lags used. Using the same value for the number of the lags for the correlation analyses for both F_s and A_p time series may not be physically justifiable. For these reasons, we have chosen to use the non-parametric tests.

3. Results

3.1 Correlation with Solar Irradiance and Geomagnetic Activity

One major difficulty of separating solar irradiance and geomagnetic signals is that the time series of F_s and A_p are not orthogonal but positively correlated to each other. This prevents a direct use of some common techniques, such as multiple linear regressions. As is shown in Table 1, their correlation coefficient (r) is stronger for some periods and weaker for others. It shows that r tends to increase with the cutoff period of the temporal filter as well. We found that the lowest correlation occurs during Jan.1968 to Dec. 2004 and the highest correlation occurs during Jan. 1958 to Dec. 2001. Low r values between F_s and A_p may provide a better chance to separate the long-term effects of solar irradiance and geomagnetic activity. In addition, previous studies found that the radiosonde data are sparse and less reliable in the tropics and in the SH prior to 1968 [*Labitzke et al.*, 2002; *Salby and Callaghan*, 2006]. For these reasons, the results reported below are primarily based upon the period from Jan. 1968 to Dec. 2004.

[Insert Table 1 here]

Figure 2 shows the correlation maps between F_s and T_a in vertical meridional cross section under six different temporal filtering conditions using all the monthly data from Jan. 1968 to Dec. 2004. In Figure 2a, the correlations are calculated without any detrending or smoothing. Positive solar signals are found in the tropospheric equator to middle latitudes with $r_{\max}$ = 0.3 (at 40°S, 700 hPa). While the correlation coefficients are smaller, they are statistically significant with a confidence level above 95%, in the region around from 40 – 60°, 300 – 850 hPa in both hemispheres. Weak, statistically non-significant correlations are found in the subtropics of the stratosphere (~10 – 30°, 30 hPa in both hemispheres). Figure 2b shows that, when T_a is detrended, the stratospheric F_s signals increase and become statistically significant in the subtropics, while the signals in the troposphere reduce slightly. Figure 2c shows that *r* increases 50% (from 0.3 to 0.45) when both F_s and T_a are low-pass filtered with a 12-month cutoff period. Figures 2(d–f) show that *r* increases with the cutoff period of the low-pass filter and $r_{\max}$ = 0.82 is found at the centre of the SH Ferrell cell (–40°, 700 hPa) when the cutoff period is taken as 5 years. For all six cases, positive correlations predominate, indicating a warmer atmosphere during solar maxima. Figures 2(c;f) suggest that solar irradiance may contribute up to 15% of inter-annual variation of T_a at mid-latitudes of the troposphere and may account for up to 60% of inter-decadal variation of T_a in the same regions, while 5 to 40% of inter-annual to inter-decadal variations of T_a can be accounted for in the sub-tropical stratosphere. However, it is worth noting that, despite a large increase in *r* due to increases in the cutoff periods of the low-pass filter, the regions with confidence level above 95% can only be found around the Ferrell cell of the NH.

[Insert Figure 2 here]

As a sensitivity test, we performed the same correlation analysis as Figure 2 but using data from Jan. 1958 instead of Jan. 1968. The resulting correlation pattern (Figure 3) becomes less symmetric about the equator in both the troposphere and stratosphere, with slightly lower values of *r* found in the SH. This is likely to be because of poorer data quality and quantity in the SH prior to 1968. Because the number of samples has increased, larger than 95% confidence levels are able to be established over a much broader area of the troposphere. Confidence levels above 95% covers the entire Ferrell cells in both hemispheres and the edges of the Hadley cells. However, in the stratosphere, the region with confidence levels above 95% remains virtually the same. Further sub-sampling analysis suggests that the F_s signals at mid-latitudes of the troposphere and in the subtropical stratosphere are rather robust while those in the tropics are less stable. They become weaker if 1958–2001 data are used and even negative if only 1979–2001 data are employed. The unstable F_s signals in the tropical troposphere probably signify a strong influence of ENSO in this region.

[Insert Figure 3 here]

Figure 4 illustrates an example of the temporal evolution of the correlations shown in Figure 2. Figure 4a;b;c;d shows the time series of F_s, the monthly, zonally averaged T_a from the NH mid-latitude (35–55°N, 850 – 300 hPa) and from the SH mid-latitude (35–45°S, 850 – 300 hPa) troposphere, detrended and smoothed T_a from both sites and the trends which are subtracted, respectively. Figure 4c shows that the amplitudes of T_a are between 0.15 – 0.35°C, with peaks / valleys approximately at maxima / minima of the solar cycle, respectively. These changes reflect a gradual drift of the temperature anomaly that tracks F_s at time scales above ~5 years.

[Insert Figure 4 here]

Figure 5 shows the same as Figure 2, but for the correlations between A_p and T_a. Without smoothing or detrending (Figure 5a), weak but significant positive A_p signals are found in the stratosphere, with the strongest A_p signal in the sub-tropical to mid-latitudes of the SH stratosphere (20–40°, 30–100 hPa) and in the Arctic stratosphere (55–75°, 30–50 hPa). With detrending and increased size of filtering windows, both the correlation coefficient and confidence levels increase. Positive correlations cover nearly the entire stratosphere when a 3 to 5-year cutoff period is applied (Figure 5e;f), except for the Antarctic polar region where missing values of T_a exist. The values of r in those affected regions are in the range of 0.1–0.2 when no filtering is applied (Figure 5a), and become as high as 0.84 when a 5-year cutoff period is applied (Figure 5f). In comparison to Figure 2 and 3, the correlations between A_p and T_a in stratospheric regions are generally higher than those between F_s and T_a, generally with a confidence level of 95% or above, suggesting possible stronger geomagnetic influence. Overall, positive correlations predominate, indicating that the stratosphere is statistically warmer during the periods where geomagnetic activity is high. In terms of the magnitude, the values of r suggest A_p may account for up to 10% of the inter-annual variation (Figure 5c) and up to 60% of the inter-decadal variation of T_a (Figure 5f) in these stratospheric regions, which is slightly higher than those accounted for by F_s (see Figures 2 and 3).

[Insert Figure 5 here]

As a sensitivity test, we performed the same correlation analysis as Figure 5 but using data from Jan.1958. The results are shown in Figure 6. Although the general spatial pattern remains the same as that of Figure 5, the values of r and confidence levels reduce considerably (by 30–50%). As is shown in Table 1, during this extended time period, the correlation between A_p and F_s is high. It is not clear why the correlation in the stratosphere is weakened rather than strengthened given the higher correlation between A_p and F_s during this longer data period. By performing the same correlation analysis using other different starting /ending times, a similar pattern emerges but with higher r and confidence values; this suggests the pattern shown in Figure 5 is relatively stable. Overall, the most robust A_p signals are the positive correlation regions in the SH subtropical and the Arctic stratosphere.

[Insert Figure 6 here]

3.2 Effects of Trend and Volcano Eruptions using Composite Analysis

The stratospheric subtropical F_s and A_p signals shown figures 2–6 are likely to be contaminated by the pronounced heating episodes associated with aerosol injections following volcanic eruptions. With three major eruptions having taken place during 1958–2001, and two of them (El Chichón and Mt. Pinatubo) occurred during the descending phase of the 11-year solar cycle, there is a chance to misattribute volcanic signals to solar irradiance or geomagnetic activity signals. To investigate such a possibility, we carried out a composite analysis by both including and excluding the data during the 2-years following a major volcanic eruption. Possible influence of the long-term trends was also examined by both keeping and removing the trends.

Figure 7 shows the averaged temperature anomaly (T_a) differences between westerly and easterly QBO (a1-a4), high and low solar irradiance (b1-b4), and high and low geomagnetic activity (c1-c4), respectively, using the data period from Jan. 1968 to Dec.2004. The analyses shown in the 1st and 3rd (or 2nd and 4th) rows include (or exclude) the data during the 2-years following a major volcanic eruption, while those shown the 1st and 2nd (or 3rd and 4th) rows also keep (or remove) the long-term trends.

Statistically significant T_a differences (ΔT_a) between westerly and easterly QBO appear predominantly in the stratosphere (see a1 to a4 of figure 7). The magnitudes of T_a differences are in the range of −1.2 to 1.5 K, which is the largest among the three signals (*i.e.* the QBO, F_s and A_p) examined and comparable to the interannaual variation of T_a [*Salby and Callaghan*, 2006]. Positive QBO signals are noticeable in the tropical upper troposphere to the lower stratosphere between 10°S to 10°N, 50–200 hPa, and at mid-latitudes, where two positive regions near 30–50 hPa, one located at ~20–60°N and another at ~20–40°S, are observed. There are two negative regions near the tropopause directly beneath those positive regions. The stratospheric mid-latitude positive-negative regions are broadly symmetric across the equator and such a pattern is known to be associated with the QBO-induced meridional circulation in temperature [*Crooks and Gray*, 2005; *Randel et al.*, 1999]. A strong negative regime is apparent in the Arctic stratosphere, particularly when the T_a time series are not detrended (30–300 hPa, see a1 and a2). Detrending reduces the magnitude of ΔT_a in the stratosphere by ~ 0.6 K in the tropics, ~ 0.8 K in the Arctic, and only ~ 0.1 K in the subtropics to mid-latitudes (comparing a3 to a1, and a4 to a2). The temperature differences increase slightly in magnitude overall (~ 0.1–0.2 K) if the data affected by volcanic eruptions are excluded (comparing a2 to a1, and a4 to a3). Detrending or excluding volcanic contamination causes little change in the confidence levels of the QBO signals, thus in the general pattern of the QBO signals in T_a.

Statistically significant, positive T_a differences between high and low F_s appear in both the stratosphere and troposphere, and their spatial pattern is broadly symmetric about the equator (see b1 to b4 of figure 7). No F_s signal is visible in the polar regions. These features are consistent with those derived from linear correlation (see figures 2 and 3). The average T_a differences are in the range of 0.1–0.4 K at mid-latitudes in the troposphere, and in the range of 0.1–0.6 K in the stratospheric subtropics to mid-latitudes. Detrending causes a measurable amount of ΔT_a increase in the troposphere (by ~ 0.1 K) and a negligible amount of ΔT_a change in the stratosphere (comparing b3 to b1, and b2 to b4 in figure7). Excluding the data contaminated by volcanic eruptions results in a measurable amount of ΔT_a reduction in the stratosphere (by ~ 0.2 K) but no change of ΔT_a in the troposphere (comparing b2 to b1, and b3 to b4 of figure7).

Statistically significant, positive T_a differences between high and low A_p appear in the subtropics to mid-latitudes and in the Arctic region of the stratosphere (see c1 to c4 of figure 7). The temperature differences are in the range of 0.1–0.7 K, with the largest temperature difference found in the SH stratospheric subtropics to mid-latitudes (~0.7 K). Such A_p signals are about 0.3–0.4 K smaller in the NH than their SH counterparts, making the A_p signature in T_a asymmetric about the equator. Detrending halves the temperature difference in the Artic stratosphere (from 0.5–0.6 K to 0.2–0.3 K) and contributes less than 0.1 K increases in ΔT_a in the NH sub-tropics to mid-latitudes (comparing c3 to c1, and c2 to c4 of figure7). Excluding the data contaminated by volcanic eruptions results in ~0.2 K reduction in ΔT_a in the stratospheric sub-tropics to mid-latitudes and 0.1 K in the Arctic stratosphere (comparing b2 to b1, and b3 to b4 in figure7).

Figure 7 suggests that, in the lower stratosphere (50–100 hPa), the effects of solar irradiance and geomagnetic activity may be comparable to each other, particularly in the SH tropics to mid-latitudes, while at similar latitudes of the middle stratosphere (30–50 hPa), the response to solar irradiance is larger. Such differences account for about 10–30% of the inter-annual variation of T_a in these stratospheric regions. In the Arctic middle stratosphere (60 –80°, 30 hPa), T_a differences between high and low A_p are statistically significant and larger than those related to solar irradiance, suggesting stronger geomagnetic influences in the polar region. In the troposphere, solar irradiance alone accounts for about 10–30% of the inter-annual variation of T_a, while the T_a differences due to geomagnetic activity are much smaller (± 0.2 K at most). The tropospheric A_p signature (significant at a 95% confidence level) appears only in the Arctic, in the case where T_a is detrended and the data contaminated by volcanic eruptions are excluded. Figure 7 also suggests that the contaminations caused by volcanic eruptions are relatively small, though they account for 0.1–0.2 K average ΔT_a increase in the stratosphere between high and low F_s (or A_p). Thus, the positive temperature anomalies resulting from volcanic eruptions do not change the general patterns of solar irradiance and geomagnetic activity signals in T_a. While the long-term trends may have stronger influence on the QBO and geomagnetic activity signals in the NH polar regions, their influence in the extra-tropical regions and on F_s signals is small.

The results presented in this and previous sections suggest positive responses of the atmospheric temperature anomaly to both solar irradiance and geomagnetic activity. The primary responses to solar irradiance occur in the tropospheric middle latitudes and the subtropical stratosphere, while geomagnetic activity responses occur mostly in the stratosphere. As figure 7 shows that the QBO accounts for the largest amount of inter-annual variation in T_a, it is useful to examine how the F_s and A_p signals shown in this section will be redistributed according the equatorial QBO phases. To achieve this and to reveal possible non-linear responses of T_a to solar irradiance and geomagnetic activity, the next section separates the data according to the phases of the QBO, solar irradiance and geomagnetic activity.

3.3 F_s and A_p signals under different sub-sampling

To represent the inter-annual variations, in the correlation analyses shown below, a 12-month cutoff period is applied to all time series involved. To focus on the temperature anomaly responses to solar irradiance and geomagnetic activity, the data during the 2-years following a major eruption are excluded.

3.3.1 Sub-sampling according to the QBO phases

Figure 8 shows the correlations between F_s and T_a (the 1st row), and A_p and T_a (the 2nd row), for all data (the 1st column), when the QBO is westerly (the 2nd column), when the QBO is easterly (the 3rd column).

The first row of Figure 8 shows that F_s signals mostly appear in the middle latitude troposphere and the subtropical stratosphere when all the data are used. When the data are sub-sampled according to the phases of the QBO, F_s signals switch between the stratosphere and the troposphere depending on the QBO phases. In the troposphere, F_s signals are stronger (or weaker) when the QBO is westerly (or easterly); in the stratosphere, the opposite holds. In the troposphere, mid-latitude F_s signals associated with the westerly phase of the QBO are robust ($r_{\max}$ = 0.54, statistically significant at the 95% confidence level). Further analysis suggests that these tropospheric signals dominate in the months of June to August (not shown). In the stratosphere, subtropical to mid-latitudes F_s signals associated with the easterly QBO is highly robust ($r_{\max}$ =

0.57, statistically significant at the 99% confidence level). These F_s signals appear slightly stronger in the NH than in the SH, but can be stated as broadly symmetry about the equator. In the NH polar region, no robust F_s signals are detected.

The second row of Figure 8 shows that the overall A_p signature is asymmetric about the equator; stronger signals detected in the SH than in the NH. When all the data are included, the signals primarily appear in the SH subtropical to mid-latitude lower stratosphere, and in the Arctic stratosphere. In comparison to F_s signals, the A_p signals are modulated by the phases of the QBO in a quite different way. Robust A_p signals are mostly found in the subtropical stratosphere for the westerly QBO phase, and A_p signals remain stronger in the SH than the NH. When the QBO is westerly, A_p signals in the NH stratosphere appear in the region of 5–20°, 30–50 hPa and extend polewards and downwards in the region of 0–40°, 50–200 hPa, while, in the SH stratosphere, the signals appear in the region of 10–50°, 30–100 hPa. In the troposphere, however, no A_p signal can be found. When the QBO is easterly, weaker and isolated positive A_p signals appear in the lower stratospheric tropics, while negative A_p signals appears in the SH mid-latitude troposphere. Indistinguishable positive A_p signals in the Arctic stratosphere are found for both westerly and easterly QBO phases.

[Insert Figure 8 here]

3.3.2 Sub-sampling according to the intensity of Fs

Figure 9 shows the correlations between the QBO and T_a (the 1st row), and A_p and T_a (the 2nd row), for all data (the 1st column), when F_s is high (the 2nd column), and when F_s is low (the 3rd column).

The first row of Figure 9 shows that slightly stronger positive and negative QBO signals are found when F_s is low than those when F_s is high. When F_s is low, enhanced positive QBO signals are found in the equatorial to mid-latitude stratosphere and negative QBO to T_a correlations are found in the Arctic stratosphere. By performing the same correlation analysis using different periods, we found that these solar irradiance-dependent QBO correlation patterns are rather robust. That is, slightly stronger QBO signals tend to appear when F_s is low.

[Insert Figure 9 here]

The second row of Figure 9 shows that the effects of solar irradiance on A_p signals in T_a. When all data are included, similar to those shown in the 3rd column of figure 7, the A_p signals are asymmetric about the equator, primarily appearing in the SH stratospheric subtropics to mid-latitudes, and in the Arctic stratosphere. When F_s is high, A_p signals in the stratospheric subtropics and mid-latitudes are enhanced and become symmetric about the equator ($r_{\max}$ = 0.49, significant at a 99% confidence level). This indicates that up to 23% of inter-annual variation of T_a in the region can be explained by the variation of A_p during the years when solar irradiance is high. Weaker but robust negative A_p signals are found in the troposphere (20–30°, 200–1000 hPa), located directly under those positive signals, implying negative influence of geomagnetic activity on the Hadley circulation. When F_s is low, positive A_p signals appear in the Arctic stratosphere with $r_{\max}$ = 0.43, accompanied by negative A_p signals at mid-latitudes in the stratosphere with $r_{\min}$ = 0.35, suggesting a warmer than average Arctic stratosphere is accompanied by a cooler than average counterpart in the stratospheric mid-latitudes. A_p signals in the tropical and subtropical stratosphere are weak and no A_p signal can be found in the troposphere.

3.3.3 Sub-sampling according to the Geomagnetic Ap index

Figure 10 shows the correlations between the QBO and T_a (the 1st row), and F_s and T_a (the 2nd row), for all data (the 1st column), when A_p is high (the 2nd column), and when A_p is low (the 3rd column).

[Insert Figure 10 here]

The first row of Figure 10 shows that stronger QBO signals are associated with low geomagnetic activity, notably at the lower stratospheric tropics and the stratospheric mid-latitudes. In the Arctic stratosphere, the correlation coefficients are approximately equal (–0.35) for all three cases: all data, when A_p is high and when A_p is low. In the troposphere, statistically significant (at a 95% confidence level and above) positive QBO signals are found at the centre of the SH Ferrell cell (40°S) and negative QBO signals are found directly above, only when A_p is high.

The second row of Figure 10 shows that the spatial patterns of the correlations remain symmetric about the equator in the both stratosphere and troposphere for all three cases: all data, when A_p is high and when A_p is low. When A_p is high, enhanced F_s signals appear in the stratospheric subtropics with r values increased by 20 – 30% and the confidence levels increased from 95% to 99%. Such behavior of the F_s signature is somehow similar to the case when the data were sub-sampled according to the QBO phases (see 1st row of figure 8). In the troposphere, however, the F_s siganls are found in the poleward part of the Ferrell cells when A_p is high, and between the Hadley cells and the Ferrell cells, when A_p is low. Thus, the primary regions of T_a responses to F_s in the troposphere tend to shift towards the equator when A_p is low and towards the poles when A_p is high.

4. Discussions

There are two reasons that we chose to apply simple correlation and composite analysis rather than multi-linear regression (MLR). Firstly, F_s and A_p are correlated to each other, as shown in Table 1, while MLR requires that the regressing time series are not (or at least are only weakly) correlated to each other. Secondly, although MLR may have the advantage of handling multiple variables, it remains hard to guarantee that the variables used can actually account for all the influential processes. Failure to account for other variables or processes can potentially lead to wrong interpretations, as the predicted responses to the *recognized* variables are the results of the proposed multi-linear model, which may not necessarily represent the true physical processes. In particular, if the governing processes are non-linear, a MLR model with many variables included can be worse than a simple one as there are many degrees of freedom to fit the data.

The influences of solar irradiance are mostly positive in both the stratosphere and troposphere, and the signals are robust in the tropospheric mid-latitudes and in the stratospheric subtropics. In the troposphere, the locations of the mid-latitude positive F_s signals are in good agreement with the findings of *Haigh* [2003], *Crooks and Gray* [2005] and *Gleisner and Thejll* [2003], but differ from those of *Salby and Callaghan* [2006], who used NCEP/NCAR reanalysis and found almost no response in the same regions. We have found that most of the warming signal associated with F_s in the troposphere lies on the poleward side of the Ferrell cells, suggesting a weakening of its upward branch. This is consistent with the findings of *Gleisner and Thejll* [2003] and *Haigh* [2003] where the NCEP/NCAR re-analysis was used. The magnitude of temperature responses associated with F_s (~0.4 K), however, are larger than GCM simulations using an observed solar energy spectrum and the associated ozone changes (~0.1 K) [*Haigh*, 1999a; *Shindell et al.*, 1999; *Shindell et al.*, 2001]. Sub-sampling further suggests that solar irradiance signals are broadly symmetry about the equator and tend to migrate around the Ferrell cells and the poleward part of the Hadley cells. These observations agree well with recent observational findings of *Salby and Callaghan* [2006], and support the previously proposed connection between solar irradiance and temperature differences between solar maximum and minimum years. *Labitzke* [2001] suggested that the positive temperature differences between solar maximum and minimum years could be explained to some extent by an intensified Hadley circulation, *i.e*. intensified downward motion in the upper troposphere during solar maximum.

In the stratosphere, the locations of the positive signals in the subtropics of each hemisphere at around 10°–30° and 30–100 hPa agree with those of *Crooks and Gray* [2005], *Hood* [2004] and *Salby and Callaghan* [2006]. However, a negative temperature response to F_s was found at high latitudes of both hemispheres by *Crooks and Gray* [2005] and *Keckhut et al.* [2005], while *Hood* [2004] and *Scaife et al.* [2000] reported positive responses in the same regions. Here, we found no statistically significant temperature responses to F_s at high latitudes, agreeing with *Salby and Callaghan* [2006]. In terms of the magnitude of the temperature responses, ~0.5 K increases are detected by this study (see figure 7), which is comparable to the findings of *Hood* [2004], *Keckhut et al.* [2005] and *Salby and Callaghan* [2006], but slightly smaller than that detected by *Crooks and Gray* [2005]. *Crooks and Gray* [2005] used ERA-40 reanalysis for the period of 1979–2001 and found ~0.75 K increases in the SH when two years following major volcanic eruptions are excluded from their linear regression analysis. The responses found by this study are also smaller than those studies in which the composite analysis or correlations were performed based upon single-calendar-month sampling at around solstice [*Labitzke*, 2001; *Labitzke*, 2003; *Salby and Callaghan*, 2006]. Thus, these differences are largely due to either the different datasets used or the analysis methods employed. It is worth noting that, although the magnitude of the temperature response is generally found to be larger in the stratosphere than that in the troposphere, a comparable amount of inter-annual to inter-decadal variation in T_a is accounted for by F_s because of the smaller inter-annual variation of T_a in the troposphere.

The results of the QBO modulation on the F_s signature (Figure 8) are also in general agreement with what has been reported by *Labitzke* [2003], who used only July and August data from NCEP/NCAR re-analysis (1968-2002). We confirm here that such QBO modulated 11-year solar cycle signals are statistically significant at inter-annual time scales as well.

In comparison to the temperature responses to solar irradiance, T_a responses to geomagnetic activity are primarily in the stratosphere, and such a signature is asymmetry about the equator. Positive A_p signals are detected in the subtropics to mid-latitudes with larger temperature responses in the SH than in the NH. Such A_p signals cannot be compared to previous studies as literally no work has been published in the area.

The temperature anomaly in the stratosphere responds to both solar irradiance and geomagnetic activity positively, reflecting warmer conditions for the lower to middle stratosphere and indicating anomalous upwelling of the Brewer-Dobson circulation. In the Arctic stratosphere, the responses to geomagnetic activity are robust and dominate over the responses to solar irradiance. The sub-sampling (figures 9) shows that such an A_p signature is enhanced when solar irradiance is low. Our seasonal analysis (not shown) further suggests that the signature appears mostly during late winter and early spring, implying the important role of NO_x descent from higher altitudes during the winter to spring seasons. In terms of statistical significance, geomagnetic activity signals achieve higher confidence levels in general than those of solar irradiance in the stratosphere.

A high level of geomagnetic activity enhances solar irradiance signals in the stratosphere and vice versa. *Haigh* [1996] argued that an increase in stratospheric temperature during solar maximum conditions leads to a strengthening of easterly winds, which penetrate into the tropical upper troposphere. The pronounced vertical bipolar structure in T_a responses to A_p over the Arctic stratosphere (see figure 7c1-c4) may provide an additional clue for such mutual-enhancement in solar influences in the atmosphere. Modeling studies show that a similar vertical bipolar structure is associated with solar irradiance, and such bipolar structure seems to enhance easterly wind anomaly in the NH extra-tropics [*Egorova et al.*, 2004]. The vertical bipolar structure associated with geomagnetic activity may play an important role dynamically by either reinforcing or blocking the F_s signature getting into the troposphere. Such a reinforcing /blocking mechanism is also evident by the sub-sampling shown in the second rows of figures 8 and 9, in which negative influence of geomagnetic activity in the Hadley cells are found, primarily when the QBO is easterly or F_s is high. Note that the sign of the A_p signals is opposite to that of the F_s signals in the same region of the Hadley cells, implying that the Hadley circulation response to solar irradiance and geomagnetic activity is complex. The effects of solar irradiance and geomagnetic activity may enhance or compensate each other, depending on the combined condition of atmospheric dynamics and relative intensity of solar irradiance and geomagnetic activity.

In the Arctic stratosphere, the signs of the F_s signals agree well with previous studies regarding solar irradiance-QBO phase modulation [*Labitzke*, 1987; *Labitzke and van Loon*, 1988; *Salby and Callaghan*, 2006], only if the sub-sampling is made seasonally (not shown). For the winter period (Dec–Feb), we found positive correlations between F_s and T_a during the westerly QBO phase with $r_{\max} = 0.33$ at 60°N, 50 hPa. The correlations are statistically significant at a 95% confidence level. Opposite correlations between F_s and T_a are found for the easterly QBO phase with $r_{\max} = -0.34$ at 70 °N, 200 hPa, but the correlations are not statistically significant at a 95% confidence level. The weaker correlations found by this study are most likely due either to the sampling methods, to the different filters used, or to data quality. Nevertheless, these results may also suggest that considerable intra-seasonal variations exist in the Arctic stratosphere. In the subtropical stratosphere, the positive F_s signals associated during easterly QBO are highly robust, but the correlation coefficients are considerably smaller than those from studies in which the correlations were performed based upon single-calendar-month sampling around the solstices [*Labitzke*, 2003; 2004].

The combined effects of radiative heating at the tropics and mid-latitudes and O_3 depletion at the higher latitudes seem to produce a stronger, cross-hemisphere anomalous dynamical response, consequently, more symmetric patterns of both F_s and A_p signals. The changing spatial patterns of F_s and A_p signals according to the QBO phase further imply the important role of dynamical coupling. Nevertheless, the mechanisms associated with the observed subtropical to mid-latitude stratospheric F_s

and A_p signals are not very clear. It is known that an increase of UV irradiance causes a higher rate of photochemical O_3 production in the stratospheric tropics and mid-latitudes. This increased ozone concentration causes higher radiative heating and hence higher temperature, primarily in the upper stratospheric lower latitudes [*Gray et al.*, 2005; *Hood*, 2004]. The direct temperature responses to the UV-O_3 photochemical processes in the lower stratosphere, however, are relatively small and cannot explain the observed solar signals in the lower stratosphere. *Kodera and Kuroda* [2002] attributed such F_s signals to dynamical responses and proposed a plausible mechanism.

Another puzzle is that, although cooling rather than warming is expected to accompany O_3 depletions by the descending NO_x (through catalytic reactions), A_p signals revealed by our statistical inferences here are mostly positive. If these positive A_p signals in the subtropics and the Arctic of the lower to mid-stratosphere are an indication of physical processes, they are likely due to *indirect* or dynamical responses, as suggested by a recent model study [*Rozanov et al.*, 2005]. The following mechanisms may be speculated for the mutual enhancement of the F_s and A_p signals in the stratosphere subtropics. High geomagnetic activity enhances NO_x productions in the thermosphere and mesosphere. In the presence of strong polar vortex conditions, NO_x descends and depletes O_3 primarily at high latitudes of the upper stratosphere [*Solomon et al.*, 1982]. Observational studies suggest stronger polar night jet tends to occur during winter under solar maximum conditions [*Kodera*, 1995; *Kuroda and Kodera*, 2002]. This provides an optimal condition for NO_x to descend; thus larger A_p signals are expected under solar maximum conditions. An increase of UV also leads to increases of equatorial upper stratospheric ozone and radiative heating, and produces, through the thermal wind relationship, an enhancement of the zonal wind in the subtropics of the winter hemisphere [*Kodera and Kuroda*, 2002]. A possible dynamical feedback is that high latitudes O_3 depletion caused by the descent of NO_x may act as an enhancement mechanism for the initial solar-UV-induced zonal wind anomaly in the subtropical upper stratosphere to propagate downward and poleward during winter. As proposed by *Kodera and Kuroda* [2002], a dynamical consequence of wind anomaly propagation is that upward propagating planetary waves are deflected poleward, decreasing planetary wave absorption. The reduced wave absorption in the extratropical upper stratosphere then induces an equatorward anomaly in the Brewer-Dobson circulation. This, in turn, produces a warmer than average anomaly in the tropical lower stratosphere, as statistically inferred by this study. Nevertheless, the complex dynamical-chemistry coupling cannot be revealed by the HadAT temperature anomaly data, which only cover the troposphere to the middle stratosphere, or by the simple statistical inference using here. Data covering the upper stratosphere and GCM experiments are inevitably required to clarify and test the precise mechanisms involved. It is worth noting that most of the middle-atmospheric GCMs do not consider the effects of geomagnetic activity. This could be a reason for disagreement between the GCM simulations and the observations regarding weaker solar signals in the SH and misrepresentation of the lower stratospheric warming in the tropics. Since planetary wave activity plays a major role in stratospheric dynamics and is most pronounced during NH winter period, it would be interesting to carry out a detailed analysis for winter seasons. Such an analysis has been carried out using ERA-40 reanalysis and the results are reported elsewhere.

The results reported here suggest an alternative interpretation of the solar-QBO relationship. Driven primarily by wave-mean flow interaction, T_a may be strongly influenced by both the QBO and Quasi-decadal variations (QDVs). The QDVs previously found in the literature may be due to the combined effects of solar irradiance (F_s) and geomagnetic activity (A_p), which, in turn, depends on solar magnetic flux. Further study is needed to understand how such multiple solar-related influences could be linked to the "downward and poleward control" mechanism [*Kodera and Kuroda*, 2002; *Kodera et al.*, 1990; *Matthes et al.*, 2004] and the dynamical coupling in the upper stratosphere between the tropics and the polar regions [*Gray et al.*, 2001].

5. Conclusions

The significant stratospheric F_s and A_p signals found in the radiosonde-based HadAT2 temperature anomaly data provide additional evidence to support the previously prescribed solar irradiance-QBO interaction [*Labitzke*, 1987; *Labitzke*, 2003; *Labitzke and van Loon*, 1988; *Salby and Callaghan*, 2006]. In this study, using linear correlation and composite analysis, we have examined the influences of solar irradiance and geomagnetic activity on the stratospheric and tropospheric temperature anomaly and their relative importance. Geomagnetic A_p signals are found primarily in the stratosphere, while solar irradiance signals are found in both the stratosphere and troposphere. Statistically, the difference between F_s and A_p signals is shown more clearly during the period when the correlations between F_s and A_p are relative low (Jan. 1968 – Dec. 2004). In terms of correlation coefficients, for the period from Jan. 1958 to Dec. 2004, the F_s signals are more stable than the A_p signals. In the subtropical to mid-latitude stratosphere, the influences of F_s and A_p are comparable in magnitude, particularly in the SH, while the confidence levels of A_p signals are higher than those of F_s. In the Arctic stratosphere, T_a shows a larger and more significant positive response to geomagnetic activity than to solar irradiance.

Temporal filtering has a large influence on the correlation coefficients. However, it has far less influence on the confidence levels. While r values may increase from 0.3 to 0.8 with an increase in the cut-off period applied for the low-pass filter, the regions where the correlation coefficients have confidence levels above 95% remain largely unchanged. Thus, caution is required when one quantifies solar influences based upon the correlation coefficients alone. The robustness of the signals needs to be carefully examined as well, especially when the serial correlation becomes are issue due to the applications of low-pass filtering.

We also show that, at inter-annual time scale, the temperature anomaly responds to solar irradiance and geomagnetic activity in different ways when the data are sub-sampled according to the phases of the QBO, to the intensity of solar irradiance or to the levels of geomagnetic activity. In general, for a given region, sub-sampling tends to strengthen the signals under one condition and weaken the signals under another. The stratospheric F_s signals are strengthened when the QBO is easterly or geomagnetic activity is high, while the stratospheric A_p signals are strengthened when the QBO is westerly or solar irradiance is high. The tropospheric solar signals are mostly related to solar irradiance alone and are enhanced when the QBO is westerly. The tropospheric regions where T_a shows relatively large statistical response to F_s include: 1) the Ferrell cells; 2) regions between the Ferrell cells and the Hadley cells. These tropospheric F_s signals tend to be fragmented under high or low geomagnetic activity. While the extra-polar stratospheric F_s (or A_p) signals tend to appear when geomagnetic activity (or solar irradiance) is high, the QBO signals, conversely, tend to be stronger when solar irradiance or geomagnetic activity is low.

One of the most interesting features found through sub-sampling is that, in the stratosphere, solar irradiance and geomagnetic activity tend to enhance each other in the extra-polar region and compensate each other in the Arctic. High geomagnetic activity enhances the F_s signals by strengthening the positive correlation between F_s and T_a in the stratosphere, while high solar irradiance seems to enhance the correlations between A_p and T_a in the subtropical to mid-latitude lower stratosphere. Such signal enhancement is made symmetrically about the equator. The anomalous increase/decrease in temperature in these regions would alter the large-scale atmospheric circulation, including the Brewer-Dobson and the Hadley circulations. The Ferrell cells, which exist in response to the transfer of energy from lower to higher latitudes by mid-latitude eddies, are identified as one of the primary regions influenced mostly by solar irradiance.

In summary, geomagnetic activity and solar irradiance interact with each other and their effects in the atmosphere may either reinforce (*e.g*. at the tropics and mid-latitudes) or compromise each other (*e.g*. high-latitudes and polar region). The reinforcement or compromising also depends on the modulating effects of atmospheric dynamics, which cause additional spatial and seasonal variations in those signals. Though physical mechanics of mutual-modulation can be extremely complex, at inter-annual time scale, atmospheric response to solar irradiance and geomagnetic activity are shown to be statistically different during different phases of the stratospheric QBO. This suggests that the QBO, and its phase in particular, may act as a mechanism to change the propagation conditions for planetary waves and as an amplifier for possible multiple solar signals in the lower part of the atmosphere.

6. ACKNOWLEDGEMENTS

We wish to thank three anonymous reviewers for their thoughtful and constructive comments, which greatly improved this paper. In particular, we are grateful to one reviewer for bringing our attention to the random-phase test method of *Ebisuzaki* [1997]. Implementing the recommended significant tests has enhanced the credibility of our results.

References

Arnold, N.F., and T.R. Robinson, Solar magnetic flux influences on the dynamics of the winter middle atmosphere, *Geophysical Research Letters, 28* (12), 2381-2384, 2001.

Baldwin, M., and T.J. Dunkerton, Quasi-biennial modulation of the southern hemisphere, *Geophysical Research Letters, 25* (17), 3343-3346, 1998.

Baldwin, M.P., L.J. Gray, T.J. Dunkerton, K. Hamilton, P.H. Haynes, W.J. Randel, J.R. Holton, M.J. Alexander, I. Hirota, T. Horinouchi, D.B.A. Jones, J.S. Kinnersley, C. Marquardt, K. Sato, and M. Takahashi, The quasi-biennial oscillation, *Reviews of Geophysics*, *39* (2), 179-229, 2001.

Boberg, F., and H. Lundstedt, Solar wind variations related to fluctuations of the North Atlantic Oscillation, *Geophysical Research Letters*, *29* (15), 1718, 10.1029/2002GL014903, 2002.

Bochnicek, J., V. Bucha, P. Hejda, and J. Pycha, Relation between Northern Hemisphere winter temperatures and geomagnetic or solar activity at different QBO phases, *Journal of Atmospheric and Terrestrial Physics*, *58* (7), 883-897, 1996.

Brasseur, G., and S. Solomon, *Aeronomy of the Middle Atmosphere*, Dordrecht, 1986.

Bucha, V., and V. Bucha, Geomagnetic forcing of changes in climate and in the atmospheric circulation, *Journal of Atmospheric and Solar-Terrestrial Physics*, *60* (2), 145-169, 1998.

Callis, L.B., R.E. Boughner, M. Natarajan, J.D. Lambeth, D.N. Baker, and J.B. Blake, Ozone Depletion in the High-Latitude Lower Stratosphere - 1979-1990, *Journal of Geophysical Research-Atmospheres, 96* (D2), 2921-2937, 1991.

Callis, L.B., M. Natarajan, and J.D. Lambeth, Calculated upper stratospheric effects of solar UV flux and NOy variations during the 11-year solar cycle, *Geophysical Research Letters*, *27* (23), 3869-3872, 2000.

Clilverd, M.A., A.A. Seppala, C.J. Rodger, P.T. Verronen, and N.R. Thomson, Ionospheric evidence of thermosphere-to-stratosphere descent of polar NO_x, *Geophysical Research Letters*, *33*, L19811, doi:10.1029/2006GL026727, 2006.

Crooks, S.A., and L.J. Gray, Characterization of the 11-year solar signal using a multiple regression analysis of the ERA-40 dataset, *Journal of Climate*, *18* (7), 996-1015, 2005.

Davis, R.E., Predictability of sea surface temperature and sea level pressure anomalies over the North Pacific Ocean, *Journal of Physical Oceanography*, *6*, 249–266, 1976.

Ebisuzaki, W., A method to estimate the statistical significance of a correlation when the data are serially correlated, *Journal of Climate*, *10*, 2147-2153, 1997.

Egorova, T.A., E. Rozanov, E. Manzini, M. Haberreiter, W. Schmutz, V. Zubov, and T. Peter, Chemical and dynamical response to the 11-year variability of the solar irradiance simulated with a chemistry-climate model, *Geophysical Research Letters*, *31*, L06119, doi:10.1029/2003GL019294, 2004.

Garrett, H.B., A.J. Dessler, and T.-W. Hill, I., Influence of solar wind variability on geomagnetic activity, *Journal of Geophysical Research*, *79*, 4603–4610., 1974.

Gleisner, H., and P. Thejll, Patterns of tropospheric response to solar variability, *Geophysical Research Letters*, *30* (13), 1711, doi:10.1029/2003GL017129, 2003.

Gray, L.J., J.D. Haigh, and R.G. Harrison, The influence of solar changes on the Earth's climate, in *Hadley Centre technical note*, pp. 82, 2005.

Gray, L.J., S.J. Phipps, T.J. Dunkerton, M.P. Baldwin, E.F. Drysdale, and M.R. Allen, A data study of the influence of the equatorial upper stratosphere on northern-hemisphere stratospheric sudden warmings, *Quarterly Journal of the Royal Meteorological Society*, *127* (576), 1985-2003, 2001.

Haigh, J.D., The impact of solar variability on climate, *Science*, *272* (5264), 981-984, 1996.

Haigh, J.D., A GCM study of climate change in response to the 11-year solar cycle, *Quarterly Journal of the Royal Meteorological Society*, *125* (555), 871-892, 1999a.

Haigh, J.D., Modelling the impact of solar variability on climate, *Journal of Atmospheric and Solar-Terrestrial Physics*, *61* (1-2), 63-72, 1999b.

Haigh, J.D., The effects of solar variability on the Earth's climate, *Philosophical Transactions of the Royal Society of London Series a-Mathematical Physical and Engineering Sciences*, *361* (1802), 95-111, 2003.

Haigh, J.D., M. Blackburn, and R. Day, The response of tropospheric circulation to perturbations in lower stratospheric temperature, *Journal of Climate*, *18*, 3672–3691, 2005.

Hinteregger, H.E., Representation of solar EUV flux for aeronomical application, *Advance in Space Research*, *139* (2), 589– 591, 1981.

Holton, J.R., and H.C. Tan, The influence of the equatorial quasi-biennial oscillation on the global circulation at 50 mb, *Journal of Atmospheric Sciences*, *37*, 2200-2208, 1980.

Hood, L.L., Effects of solar UV variability on the stratosphere, in *Solar variability and its effect on the Earth.s atmosphere and climate system*, edited by J. Pap, P. Fox, C. Frolich, H. Hudson, J. Kuhn, J. McCormack, G.R. North, W. Sprigg, and S. Wu, AGU Monograph Series, Washington D.C., 2004.

Hoyt, D.V., and K.H. Schatten, *The Role of the Sun in Climate Change*, 288 pp., Oxford University Press, New York, 1997.

Jackman, C.H., and R.D. McPeters, The effect of solar proton events on ozone and other constituents, in *Solar variability and its effect on the Earth.s atmosphere and climate system*, edited by J. Pap, P. Fox, C. Frolich, H. Hudson, J. Kuhn, J. McCormack, G.R. North, W. Sprigg, and S. Wu, AGU Monograph Series, Washington D.C., 2004.

Kodera, K., On the origin and nature of the interannual variability of the winter stratospheric circulation in the Northern-Hemisphere, *Journal of Geophysical Research-Atmospheres*, *100* (D7), 14077-14087, 1995.

Kodera, K., and Y. Kuroda, Dynamical response to the solar cycle, *Journal of Geophysical Research-Atmospheres*, *107* (D24), art. no.-4749, 2002.

Kodera, K., K. Yamazaki, M. Chiba, and K. Shibata, Downward propagation of upper stratospheric mean zonal wind perturbation to the troposphere, *Geophysical Research Letters*, *17*, 1263-1266, 1990.

Kuroda, Y., and K. Kodera, Effect of solar activity on the Polar-night jet oscillation in the northern and southern hemisphere winter, *Journal of the Meteorological Society of Japan*, *80* (4B), 973-984, 2002.

Labitzke, K., Sunspots, the QBO, and the Stratospheric Temperature in the North Polar-Region, *Geophysical Research Letters*, *14* (5), 535-537, 1987.

Labitzke, K., The global signal of the 11-year sunspot cycle in the stratosphere: Differences between solar maxima and minima, *Meteorologische Zeitschrift*, *10* (2), 83-90, 2001.

Labitzke, K., The solar signal of the 11-year sunspot cycle in the stratosphere: Differences between the northern and southern summers, *Journal of the Meteorological Society of Japan*, *80* (4B), 963-971, 2002.

Labitzke, K., The global signal of the 11-year sunspot cycle in the atmosphere: When do we need the QBO?, *Meteorol. Zeitschrift*, *12*, 209-216, 2003.

Labitzke, K., On the signal of the 11-year sunspot cycle in the stratosphere and its modulation by the quasi-biennial oscillation, *Journal of Atmospheric and Solar-Terrestrial Physics*, *66* (13-14), 1151-1157, 2004.

Labitzke, K., J. Austin, N. Butchart, J. Knight, M. Takahashi, M. Nakamoto, T. Nagashima, J. Haigh, and V. Williams, The global signal of the 11-year solar cycle in the stratosphere: observations and models, *Journal of Atmospheric and Solar-Terrestrial Physics*, *64* (2), 203-210, 2002.

Labitzke, K., and H. van Loon, Associations between the 11-year solar-cycle, the QBO and the atmosphere .1. The troposphere and stratosphere in the Northern Hemisphere in winter, *Journal of Atmospheric and Terrestrial Physics*, *50* (3), 197-206, 1988.

Labitzke, K., and H. van Loon, The QBO effect on the solar signal in the global stratosphere in the winter of the Northern Hemisphere, *Journal of Atmospheric and Solar-Terrestrial Physics*, *62* (8), 621-628, 2000.

Lean, J., Variations in the Sun’s radiative output, *Rev. Geophys. Space Phys.*, *29*, 505–536, 1991.

Lean, J.L., G.J. Rottman, H.L. Kyle, T.N. Woods, J.R. Hickey, and L.C. Puga, Detection and parameterization of variations in solar mid- and near-ultraviolet radiation (200-400 nm), *Journal of Geophysical Research-Atmospheres, 102* (D25), 29939-29956, 1997.

Matthes, K., U. Langematz, L.L. Gray, K. Kodera, and K. Labitzke, Improved 11-year solar signal in the freie universitat Berlin climate middle atmosphere model (FUB-CMAM), *Journal of Geophysical Research-Atmospheres, 109* (D6), D06101, doi:10.1029/2003JD004012, 2004.

Mayaud, P.N., *Derivation, Meaning, and Use of Geomagnetic Indices*, American Geophysical Union, Washington, DC, 1980.

Naito, Y., and I. Hirota, Interannual variability of the northern winter stratospheric circulation related to the QBO and the solar cycle, *Journal of Meteorological Society of Japan*, *75*, 925-937, 1997.

Naujokat, B., An update of the observed quasi-biennial oscillation of the stratospheric winds over the tropics., *Journal of Atmospheric Sciences*, *43*, 1873-1877, 1986.

Orsolini, Y.J., G.L. Manney, M.L. Santee, and C.E. Randall, An upper stratospheric layer of enhanced HNO3 following exceptional solar storms, *Geophysical Research Letters, 32* (12), 2005.

Pascoe, C.L., L.J. Gray, S.A. Crooks, M.N. Juckes, and M.P. Baldwin, The quasi-biennial oscillation: Analysis using ERA-40 data, *Journal of Geophysical Research-Atmospheres, 110* (D8), D08105, doi:10.1029/2004JD004941, 2005.

Randall, C.E., V.L. Harvey, G.L. Manney, Y. Orsolini, M. Codrescu, C. Sioris, S. Brohede, C.S. Haley, L.L. Gordley, J.M. Zawodny, and J.M. Russell, Stratospheric effects of energetic particle precipitation in 2003-2004, *Geophysical Research Letters*, *32* (5), L05802, doi:10.1029/2004GL022003, 2005.

Randall, C.E., D.W. Rusch, R.M. Bevilacqua, K.W. Hoppel, and J.D. Lumpe, Polar Ozone and Aerosol Measurement (POAM) II stratospheric NO2, 1993-1996, *Journal of Geophysical Research*, *103* (D21), 28361-28371, 1998.

Randel, W., F. Wu, R. Swinbank, J. Nash, and A. O'Neill, Global QBO Circulation Derived from UKMO Stratospheric Analyses, *Journal of Atmospheric Sciences*, *56* (4), 457-474, 1999.

Renard, J.B., P.L. Blelly, Q. Bourgeois, M. Chartier, F. Goutail, and Y. Orsolini, Origin of the January-April 2004 increase in stratospheric NO_2 observed in the northern polar latitudes, *Geophysical Research Letters*, *33* (11), L11801, 10.1029/2005GL025450, 2006.

Rinsland, C.P., C. Boone, R. Nassar, K. Walker, P. Bernath, J.C. McConnell, and L. Chiou, Atmospheric Chemistry Experiment (ACE) Arctic stratospheric measurements of NOx during February and March 2004: Impact of intense solar flares, *Geophysical Research Letters*, *32* (16), 2005.

Rottman, G.J., L. Floyd, and R. Viereck, Measurement of the solar ultraviolet irradiance, in *Solar Variability and Its Effects on Climate*, edited by J.M. Pap, and P. Fox, American Geophysical Union, Washington, DC, 2004.

Rozanov, E., L. Callis, M. Schlesinger, F. Yang, N. Andronova, and V. Zubov, Atmospheric response to NOy source due to energetic electron precipitation, *Geophysical Research Letters*, *32* (14), 2005.

Salby, M.L., and P.F. Callaghan, Relationship of the quasi-biennial oscillation to the stratospheric signature of the solar cycle, *Journal of Geophysical Research*, *111*, D06110, doi:1029/2005JD006012, 2006.

Seidel, D.J., and J.R. Lanzante, An assessment of three alternatives to linear trends for characterizing global atmospheric temperature changes, *Journal of Geophysical Research*, *109*, D14108, doi:10.1029/2003JD004414, 2004.

Sheeley, N.R., J.W. Harvey, and W.C. Feldman, Coronal holes, solar wind streams, and recurrent geomagnetic disturbances:1973-1976, *Solar Physics*, *49* (2), 271-278, 1976.

Shindell, D., D. Rind, N. Balachandran, J. Lean, and P. Lonergan, Solar cycle variability, ozone, and climate, *Science*, *284* (5412), 305-308, 1999.

Shindell, D.T., G.A. Schmidt, R.L. Miller, and D. Rind, Northern Hemisphere winter climate response to greenhouse gas, ozone, solar, and volcanic forcing, *Journal of Geophysical Research-Atmospheres*, *106* (D7), 7193-7210, 2001.

Siskind, D.E., G.E. Nedoluha, C.E. Randall, M. Fromm, and J.M. Russell, An assessment of Southern Hemisphere stratospheric NO_x enhancements due to transport from the upper atmosphere, *Geophysical Research Letters*, *27* (3), 329-332, 2000.

Solomon, S., P.J. Crutzen, and R.G. Roble, Photochemical coupling between the thermosphere and the lower atmosphere: 1. Odd nitrogen from 50 to 120 km, *Journal of Geophysical Research*, *87*, 7206-7220, 1982.

Thejll, P., B. Christiansen, and H. Gleisner, On correlations between the North Atlantic Oscillation, geopotential heights, and geomagnetic activity, *Geophysical Research Letters*, *30* (6), 2003.

Thiebaux, H., and F.W. Zwiers, The interpretation and estimation of effective sample size, *Journal of Applied Meteorology*, *23* (800-811), 1984.

Thorne, P.W., D.E. Parker, S.F.B. Tett, P.D. Jones, M. McCarthy, H. Coleman, P. Brohan, and J.R. Knight, Revisiting radiosonde upper-air temperatures from

1958 to 2002, *Journal of Geophysical Research*, *110*, D18105, doi:10.1029/2004JD005753, 2005.

Thorne, R.M., and T.R. Larsen, An investigation of relativistic electron precipitation events and their association with magnetic substorm activity, *Journal of Geophysical Research*, *81*, 5501-5506, 1976.

van Loon, H., and K. Labitzke, The global range of the stratospheric decadal wave. Part I: Its association with the sunspot cycle in summer and in the annual mean, and with the troposphere, *Journal of Climate*, *11* (7), 1529-1537, 1998.

Vennerstrom, S., and E. Friis-Christensen, Long-term and solar cycle variation of the ring current, *Journal of Geophysical Research*, *101*, 24727-24735, 1996.

Young, P.C., C.N. Ng, K. Lane, and D. Parker, Recursive forecasting, smoothing and seasonal adjustment of nonstationary environmental data, *Journal of Forecasting*, *10*, 57-89, 1991.

Young, P.C., C.J. Taylor, W. Tych, D.J. Pedregal, and P.G. McKenna, The Captain Toolbox. Centre for Research on Environmental Systems and Statistics, www.es.lancs.ac.uk/cres/captain, Lancaster University, UK., 2004.

Table 1. Correlation coefficients between F_s and two-month forward lagged A_p for some selected periods and filtering window sizes. The lowest correlation coefficients are highlighted.

	No smooth	12-month cutoff period	3-year cutoff period	5-year cutoff period
Jan.1958 – Dec.2004	0.2364	0.3674	0.4381	0.4800
Jan. 1968 – Dec.2001	0.1583	0.2586	0.2886	0.2879
Jan.1968 – Dec.2004	**0.1314**	**0.2174**	**0.2605**	**0.2780**
Jan.1979 – Dec.2001	0.2123	0.3396	0.3935	0.4217
Jan.1979 – Dec.2004	0.1717	0.2768	0.3460	0.3983

Figure Captions

Figure 1. Time series of monthly mean F10.7 cm solar flux (a) and geomagnetic Ap index (b).

Figure 2. Correlations between monthly F_s and T_a under six different filtering conditions during Jan. 1968 – Dec. 2004. (a) no filtering; (b) detrended, *i.e.* a high-pass filter with 50 year cutoff period; (c) a low-pass filter with 12 month cutoff period; (d) a low-pass filter with 12 month cutoff period plus detrending; (e) a low-pass filter with 3-year cutoff period plus detrending; and (f) a low-pass filter with 3-year cutoff period plus detrending, is applied, respectively. The contour values are the correlation coefficients multiplied by 10. Solid (dotted) lines are positive (negative) correlations. Dashed lines represent zero contours. Shaded areas denote confidence levels below 95% (light shaded), above 95% (medium shaded) and above 99% (dark shaded), respectively, calculated using the random phase test of *Ebisuzaki* [1997]. White areas denote no data.

Figure 3. Same as Figure 2 but the correlation analyses are performed for the period of Jan. 1958 – Dec. 2004. Shading levels are the same as for Figure 2.

Figure 4. A comparison between time series of F_s and T_a extracted from two mid-latitude tropospheric regions from Jan., 1958 to Dec. 2004. (a) Monthly F_s (black) and its UNIV smoothed signal (red); (b) Monthly zonally averaged T_a extracted from 35–55°N and 35–45°S, 300 to 800 hPa, respectively), with blue and red lines represent the T_a signals extracted from the NH / SH, respectively; (c) Detrended T_a shown in (b) and their 27-month running averages; (d) the trends which have been subtracted from T_a shown in (b).

Figure 5. Same as Figure 2 but for the correlation between A_p and T_a. Shading levels are the same as for Figure 2.

Figure 6. Same as Figure 3 but for the correlation between A_p and T_a. Shading levels are the same as for Figure 2.

Figure 7. T_a differences (ΔT_a, in the unit of Kelvin) for westerly/easterly QBO (a), high/low solar irradiance (b), and high/low geomagnetic A_p (c), respectively. The 1st and 3rd (2nd and 4th) rows, two years following a major volcanic eruptions are included (excluded). The 1st and 2nd (3rd and 4th) rows, no detrending (detrending) is applied to the T_a time series. Solid (dotted) lines are positive (negative) temperature differences and the contour values are $10\Delta T_a$ in the unit of Kelvin. Dashed lines are zero contours representing no temperature changes. Shaded areas denote temperature differences significantly different from zero at the confidence levels below 95% (light shaded), above 95% (medium shaded) and above 99% (dark shaded), respectively, calculated using Monte Carlo trial based non-parametric test. White areas donate no data.

Figure 8. The correlations between F_s and T_a (the 1st row), and A_p and T_a (the 2nd row), for all data (the1st column), when the QBO is westerly (the 2nd column), and when the QBO is easterly (the 3rd column). The contours and shading levels are the same as for Figure 2.

Figure 9. The correlations between the QBO and T_a (the 1st row), and A_p and T_a (the 2nd row), for all data (the 1st column), when F_s is high (the 2nd column), and when F_s is low (the 3rd column). The contours and shading levels are the same as for Figure 2.

Figure 10. The correlations between the QBO and T_a (the 1st row), and F_s and T_a (the 2nd row), for all data (the 1st column), when A_p is high (the 2nd column), and when A_p is low (the 3rd column). The contours and shading levels are the same as for Figure 2.

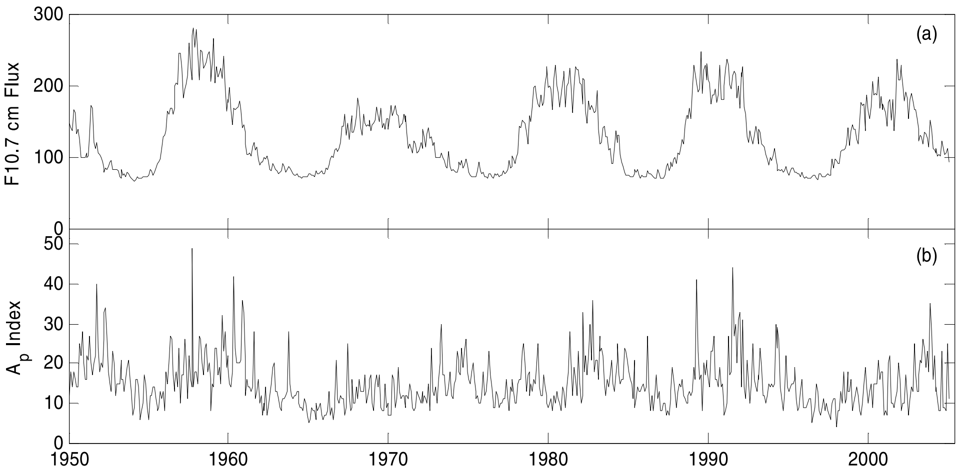
300
200
100
0
F10.7 cm Flux
(a)
50
40
30
20
10
0
A_p Index
(b)
1950
1960
1970
1980
1990
2000

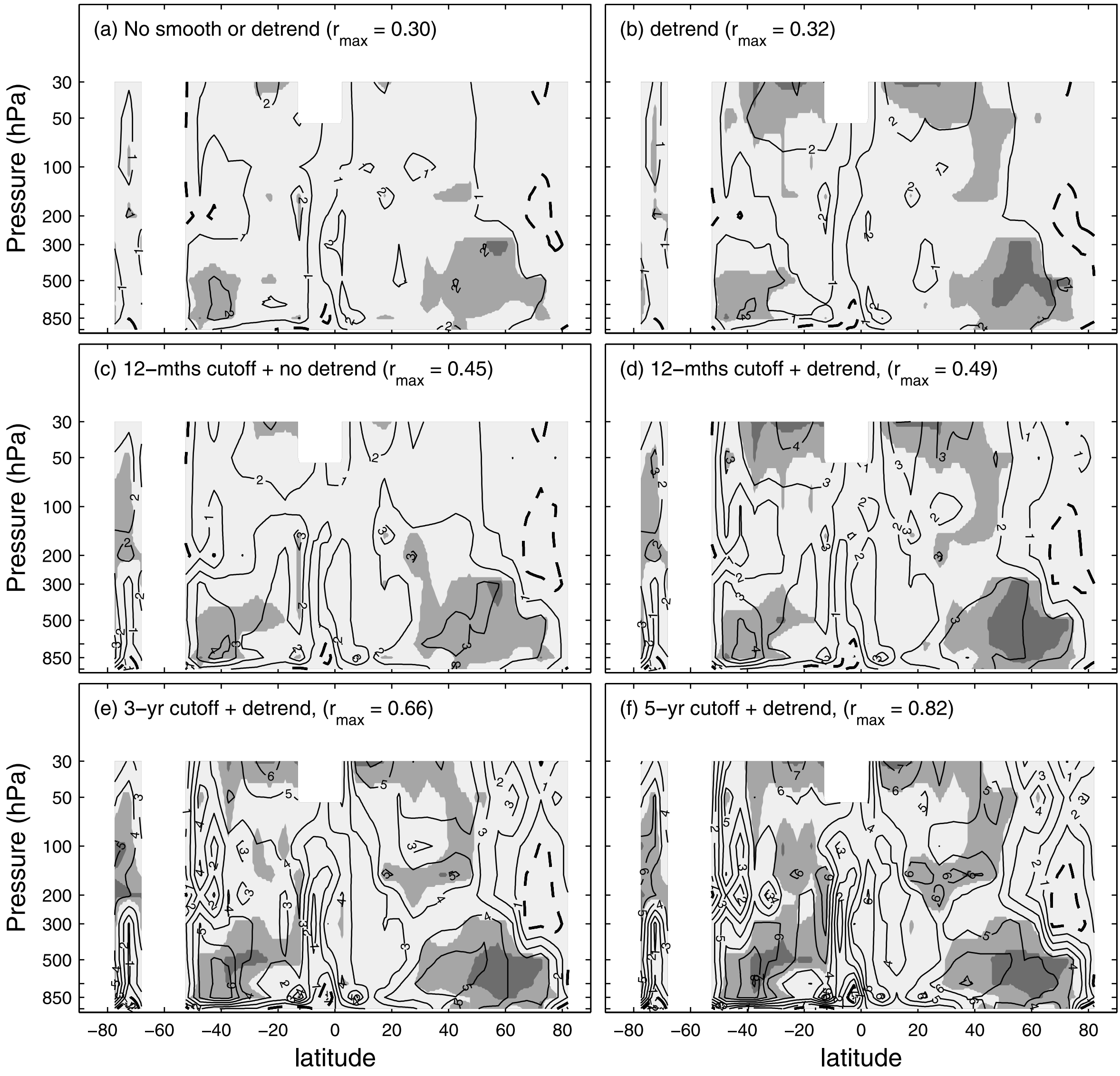

(a) No smooth or detrend (r_{max} = 0.30)
(b) detrend (r_{max} = 0.32)
(c) 12−mths cutoff + no detrend (r_{max} = 0.45)
(d) 12−mths cutoff + detrend, (r_{max} = 0.49)
(e) 3−yr cutoff + detrend, (r_{max} = 0.66)
(f) 5−yr cutoff + detrend, (r_{max} = 0.82)
Pressure (hPa)
30
50
100
200
300
500
850
latitude
−80
−60
−40
−20
0
20
40
60
80

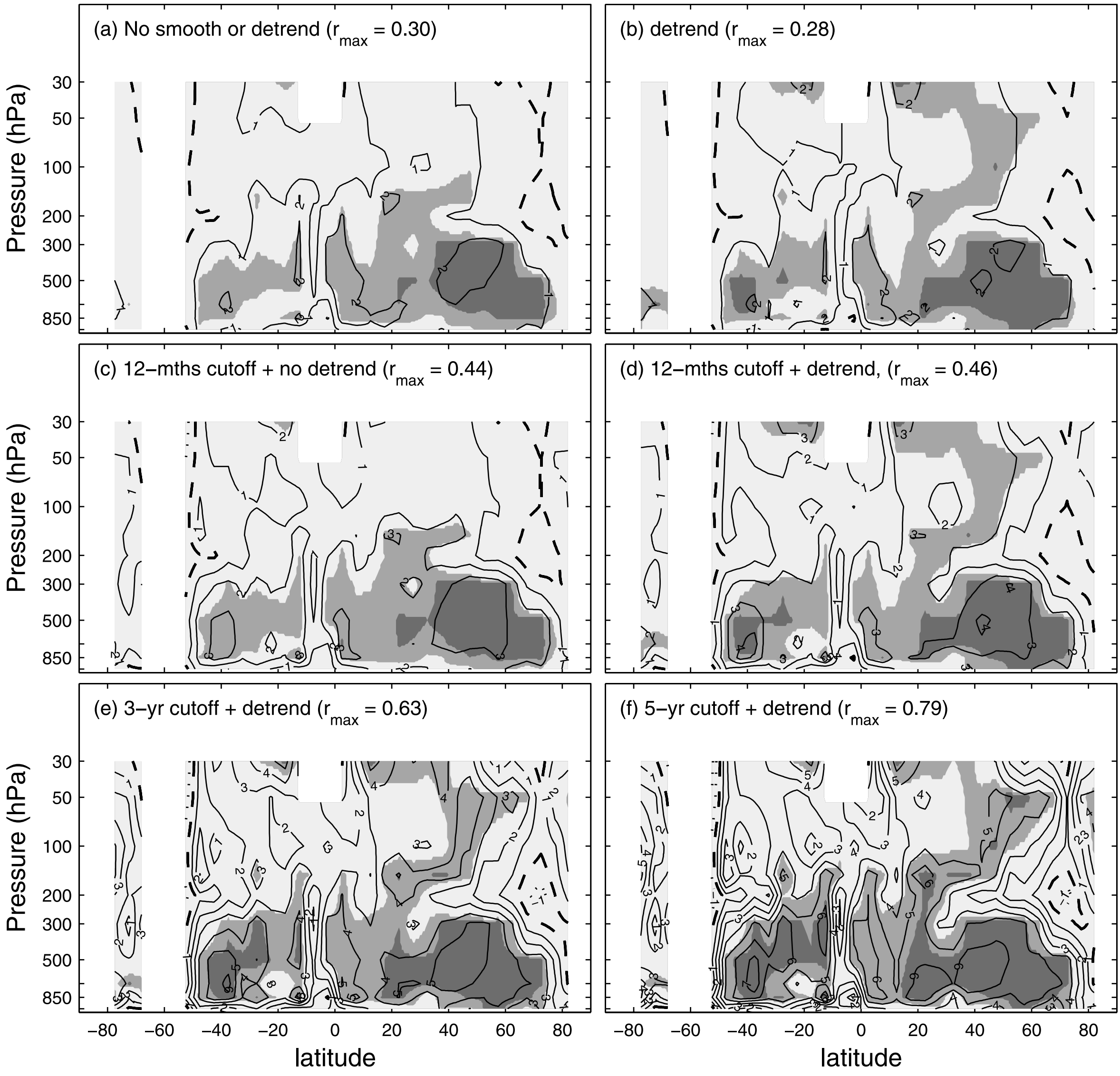

(a) No smooth or detrend (r_{max} = 0.30)
(b) detrend (r_{max} = 0.28)
(c) 12−mths cutoff + no detrend (r_{max} = 0.44)
(d) 12−mths cutoff + detrend, (r_{max} = 0.46)
(e) 3−yr cutoff + detrend (r_{max} = 0.63)
(f) 5−yr cutoff + detrend (r_{max} = 0.79)
Pressure (hPa)
30
50
100
200
300
500
850
latitude
−80
−60
−40
−20
0
20
40
60
80

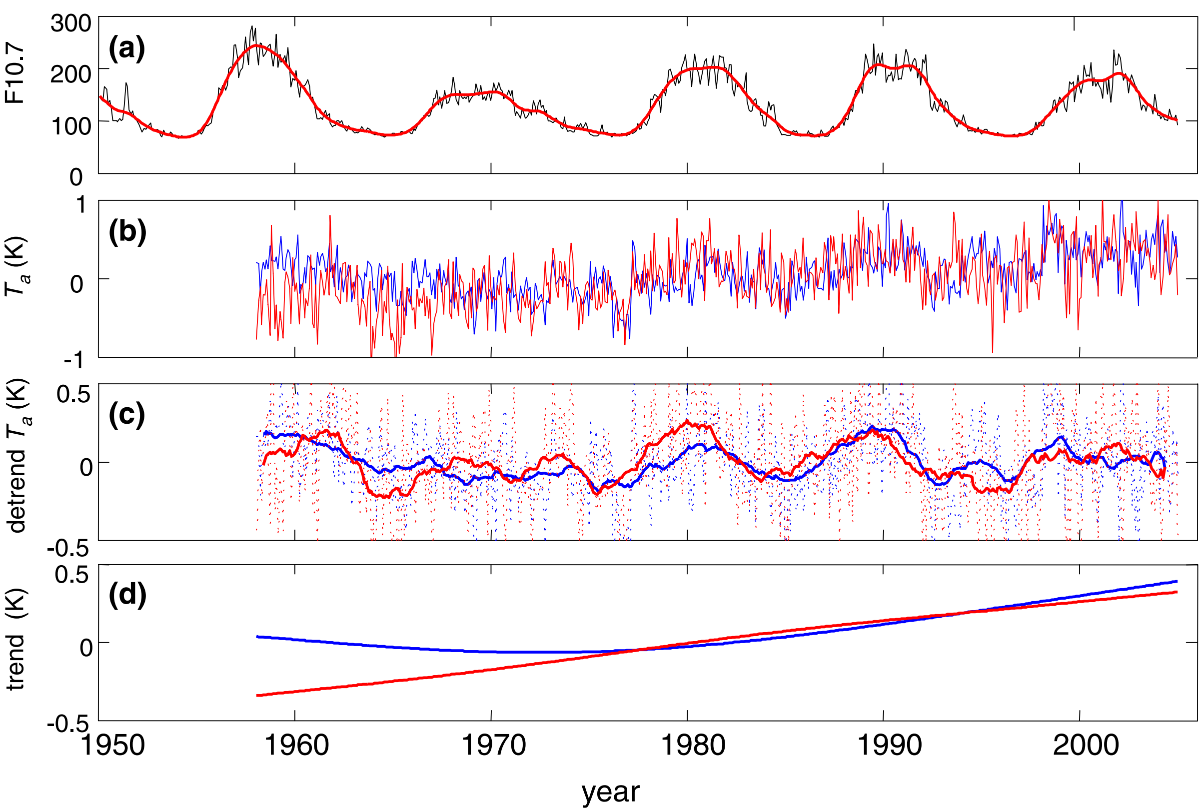

F10.7
300
200
100
0
(a)
T_a (K)
1
0
-1
(b)
detrend T_a (K)
0.5
0
-0.5
(c)
trend (K)
0.5
0
-0.5
(d)
1950
1960
1970
1980
1990
2000
year

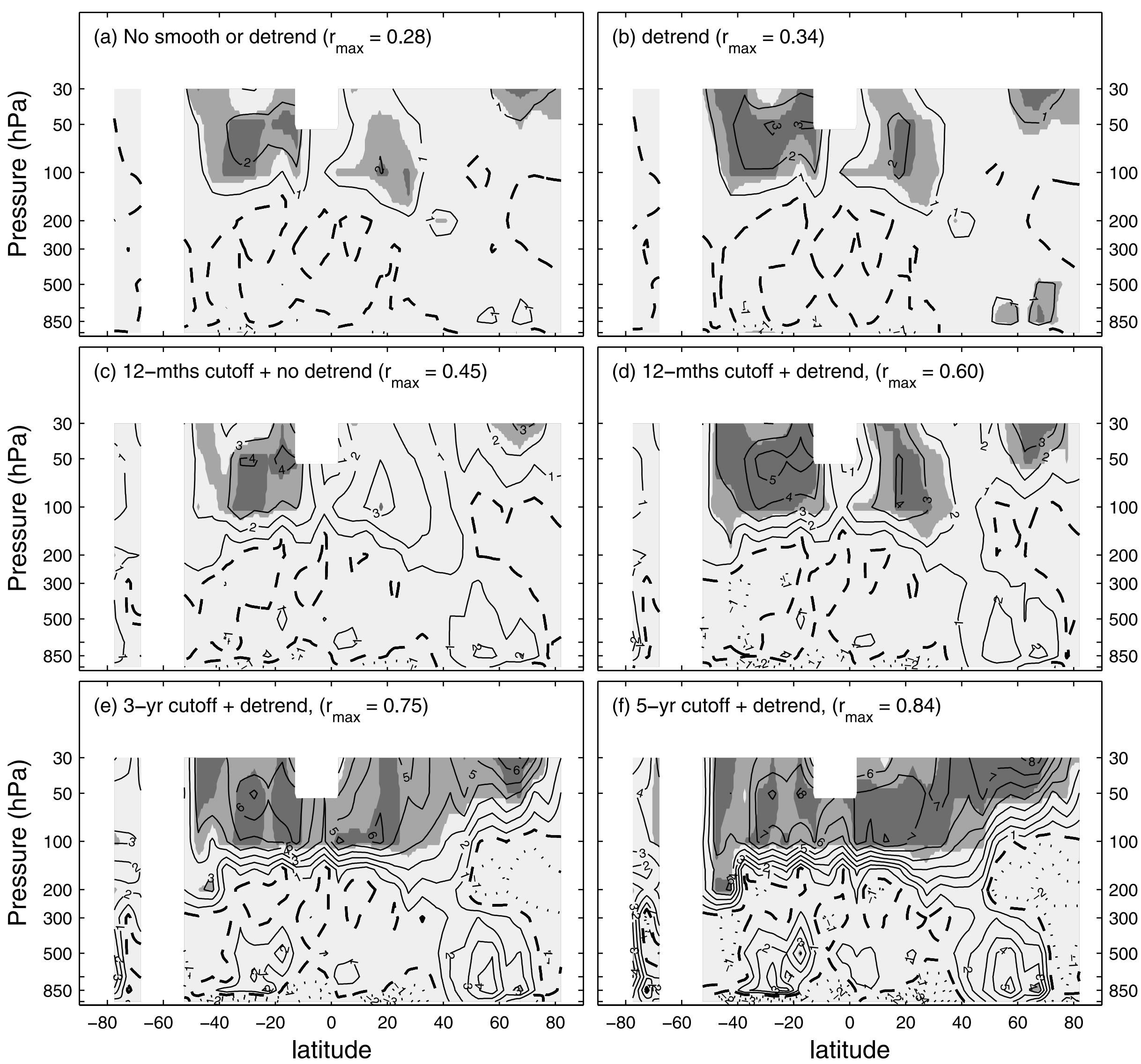
(a) No smooth or detrend (r_{max} = 0.28)
(b) detrend (r_{max} = 0.34)
(c) 12−mths cutoff + no detrend (r_{max} = 0.45)
(d) 12−mths cutoff + detrend, (r_{max} = 0.60)
(e) 3−yr cutoff + detrend, (r_{max} = 0.75)
(f) 5−yr cutoff + detrend, (r_{max} = 0.84)
Pressure (hPa)
30
50
100
200
300
500
850
−80
−60
−40
−20
0
20
40
60
80
latitude

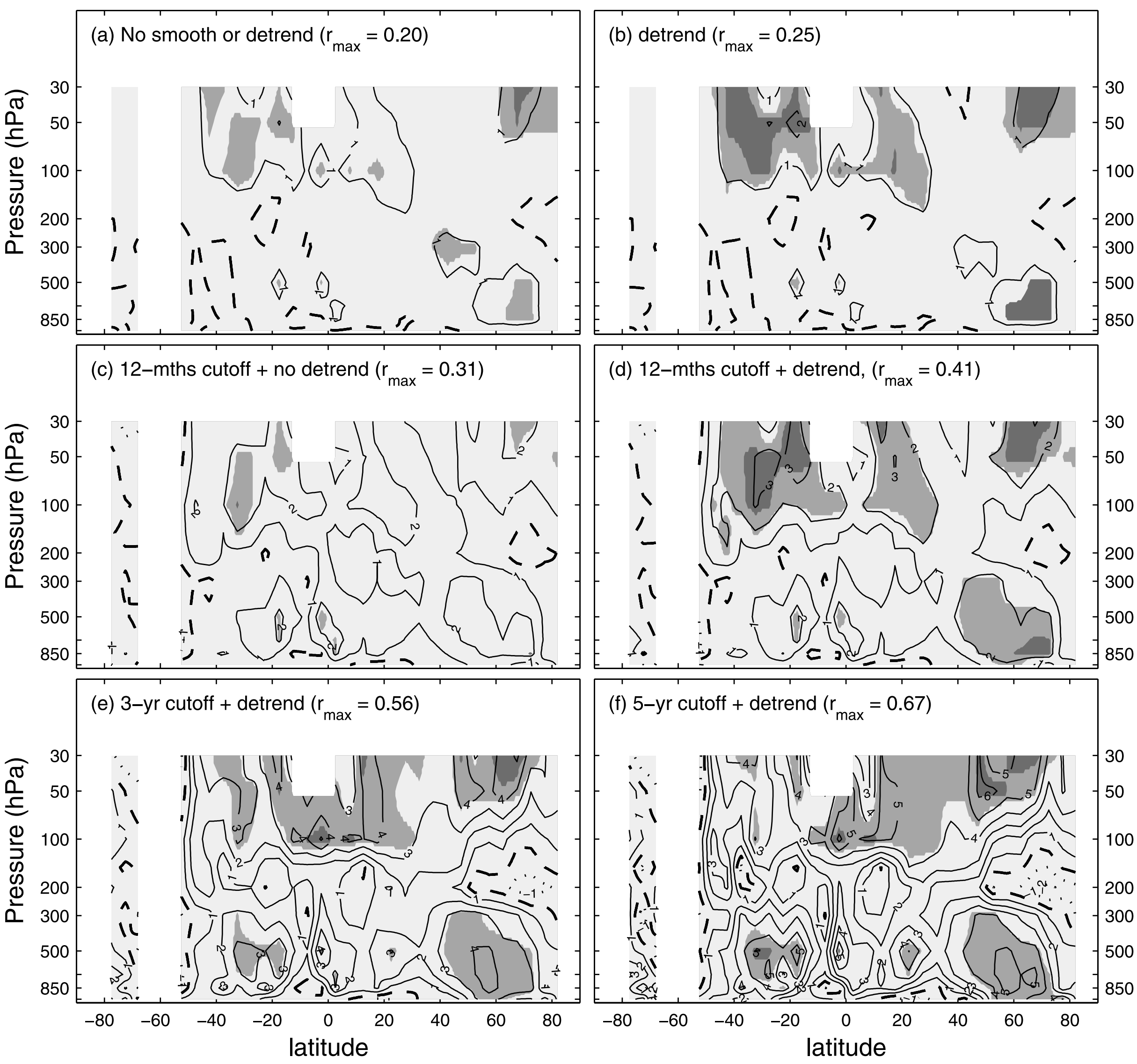

(a) No smooth or detrend (r_{max} = 0.20)
(b) detrend (r_{max} = 0.25)
(c) 12−mths cutoff + no detrend (r_{max} = 0.31)
(d) 12−mths cutoff + detrend, (r_{max} = 0.41)
(e) 3−yr cutoff + detrend (r_{max} = 0.56)
(f) 5−yr cutoff + detrend (r_{max} = 0.67)
Pressure (hPa)
30
50
100
200
300
500
850
−80
−60
−40
−20
0
20
40
60
80
latitude

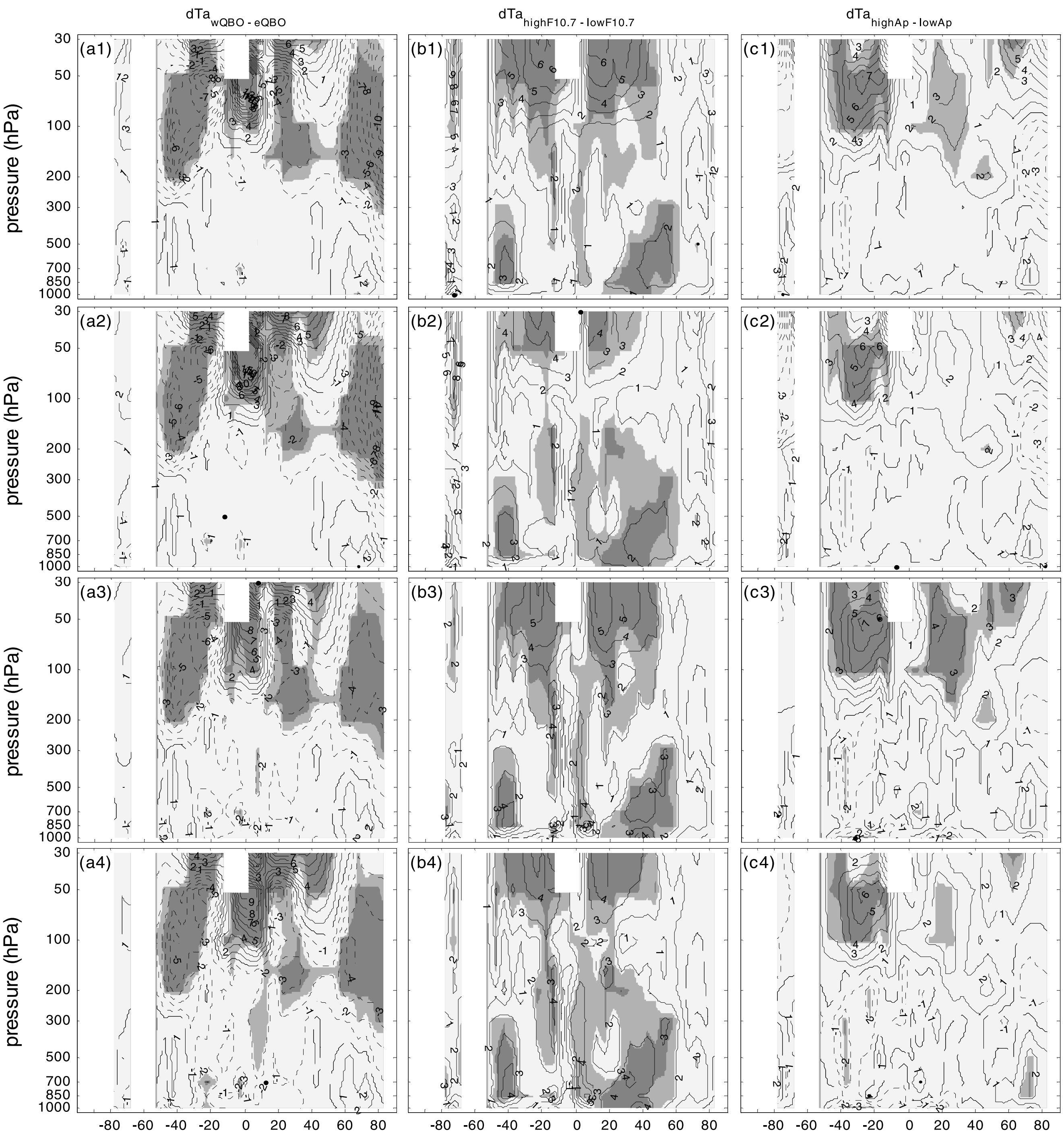

$dTa_{wQBO - eQBO}$
$dTa_{highF10.7 - lowF10.7}$
$dTa_{highAp - lowAp}$
(a1)
(b1)
(c1)
(a2)
(b2)
(c2)
(a3)
(b3)
(c3)
(a4)
(b4)
(c4)
pressure (hPa)
latitude

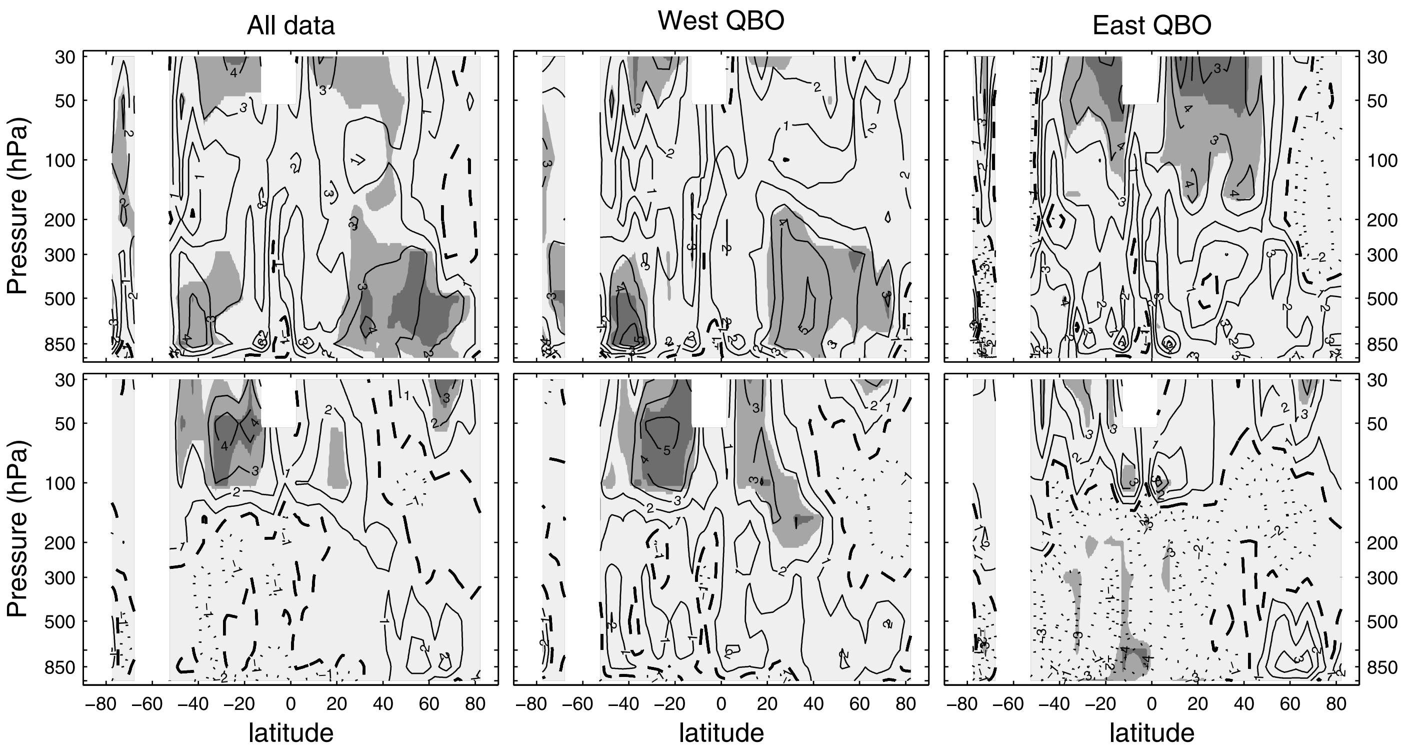
All data
West QBO
East QBO
Pressure (hPa)
30
50
100
200
300
500
850
-80
-60
-40
-20
0
20
40
60
80
latitude

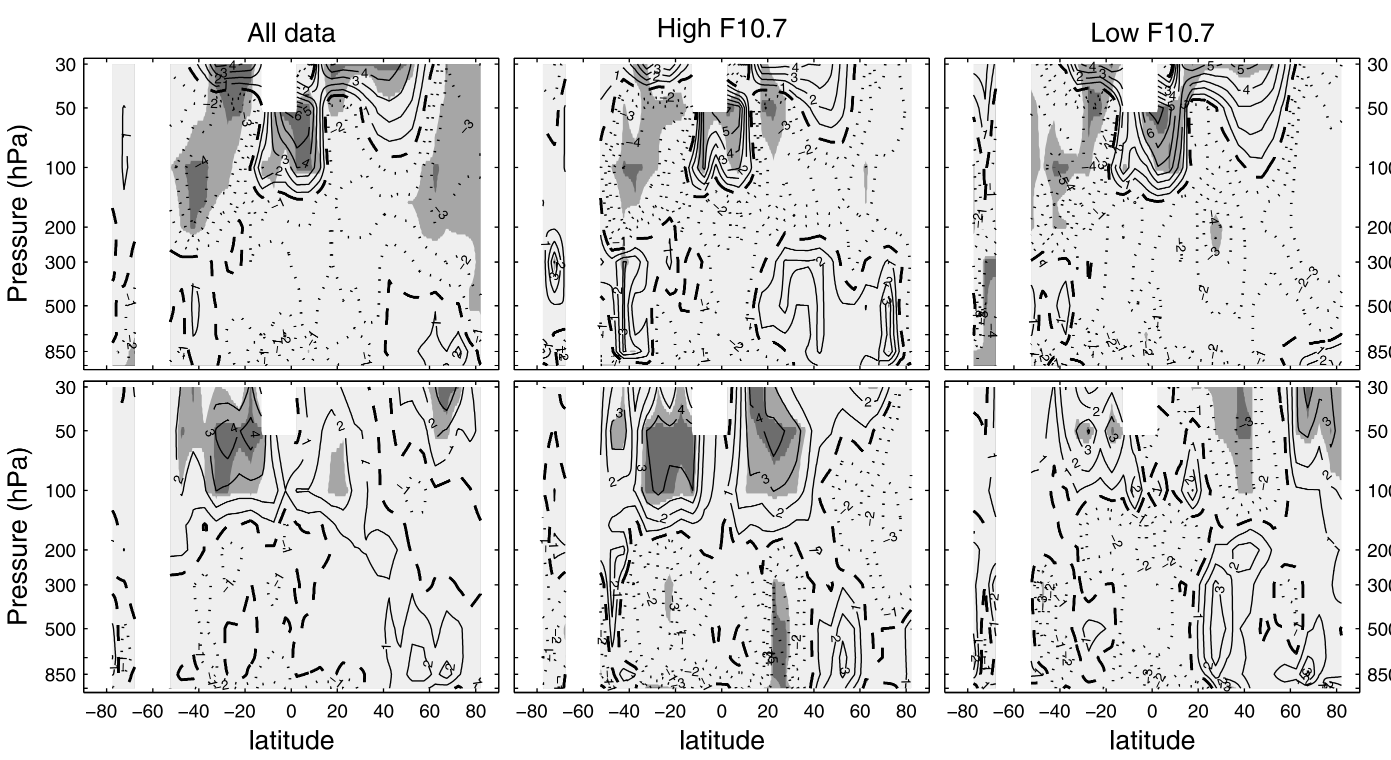

All data
High F10.7
Low F10.7
Pressure (hPa)
latitude

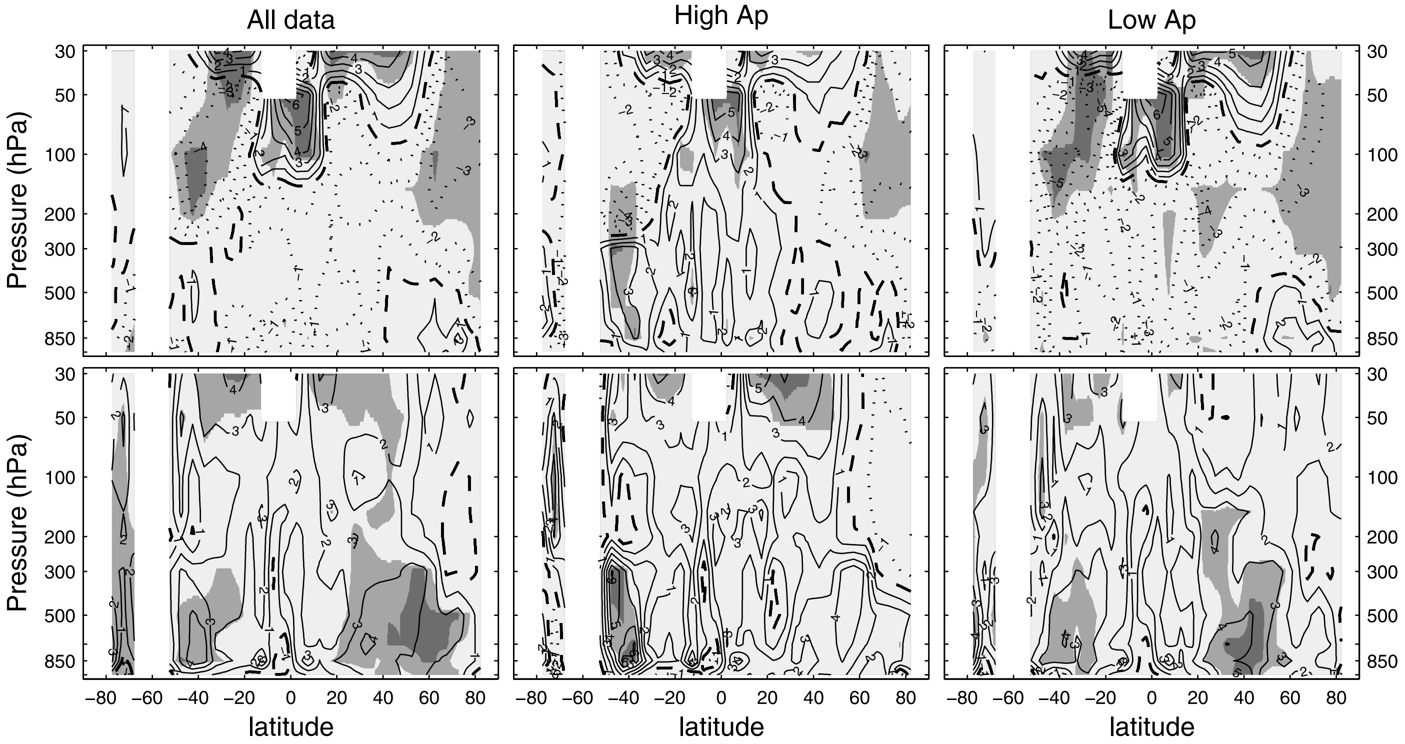
All data
High Ap
Low Ap
Pressure (hPa)
Pressure (hPa)
latitude
latitude
latitude